TUM-HEP-1062/16

Testing the low scale seesaw and leptogenesis

Marco Drewes[1], Björn Garbrecht[1], Dario Gueter[1,2,3] and Juraj Klarić[1]

[1]Physik Department T70, Technische Universität München,

James Franck Straße 1, D-85748 Garching, Germany

[2] Max-Planck-Institut für Physik (Werner-Heisenberg-Institut),

Föhringer Ring 6, 80805 München, Germany

[3] Excellence Cluster Universe, Boltzmannstraße 2,

Technische Universität München, 85748 Garching, Germany

arXiv:1609.09069v1 [hep-ph] 28 Sep 2016

Abstract

Heavy neutrinos with masses below the electroweak scale could simultaneously generate the light neutrino masses via the seesaw mechanism and the baryon asymmetry of the universe via leptogenesis. The requirement to explain both imposes constraints on the mass spectrum of the heavy neutrinos, their flavour mixing pattern and CP properties. If any heavy neutral leptons are discovered in the future, it will be possible to use a combination of different observables in order to assess whether these are indeed the common origin of the light neutrino masses and the baryon asymmetry of the universe.

Contents

1 Introduction **2**

2 Testing the seesaw mechanism **4**
2.1 The model parameters 5
2.2 Constraints from neutrino oscillation data 7
2.3 Other constraints 10
2.3.1 Normal hierarchy 12
2.3.2 Inverted hierarchy 15
2.4 Higgs contribution to heavy neutrino masses 16

3 Constraints from leptogenesis **17**
3.1 Leptogenesis from neutrino oscillations 17
3.2 Flavour mixing pattern predictions 20

4 Future improvements **28**
4.1 Direct searches 28
4.2 Heavy neutrino oscillations and CP violation 29
4.3 Neutrinoless double beta decay 30
4.4 The $\mu \to e\gamma$ rare lepton decay 32
4.5 Measurement of lepton universality violation 33

5 Conclusions **35**

A Heavy neutrino mixing angles **38**

1 Introduction

All fermions in the Standard Model (SM) of particle physics with the exception of neutrinos are known to exist with both left handed (LH) and right handed (RH) chirality. RH neutrinos could, if they exist, generate the light neutrino masses via the type I seesaw mechanism [1–6]. Traditionally it is assumed that the Majorana masses M_i of the RH neutrinos are much larger than the masses of any known particles. However, a *low scale seesaw* with Majorana masses below the electroweak scale is in perfect agreement with all known experimental and cosmological constraints [7–15]. A strong theoretical motivation for this choice is provided by the observed values of the Higgs boson and top quark masses, which lie in the region in which the SM could be a viable effective field theory valid up to the Planck scale. While the existence superheavy RH neutrinos would destabilise the Higgs mass [16], this problem is alleviated if the RH neutrinos have masses below the electroweak scale [17]. Hence, in absence of any other New Physics, a low seesaw scale M_i is required to preserve the technical naturalness of the SM with RH neutrinos. If the difference between baryon number B and lepton number L, which is conserved in the SM

due to an accidental symmetry, is an approximately conserved quantity in Nature, then the corresponding $\mathrm{U}(1)_{B-L}$ symmetry also makes comparably small Majorana masses M_i technically natural because this symmetry is exact in the limit $M_i \to 0$. This allows to explain the smallness of the light neutrino masses even for comparably large values of the neutrino Yukawa couplings Y (slightly smaller than the electron Yukawa coupling for M_i below the electroweak scale). The probably most studied model that invokes the low scale seesaw is the *Neutrino Minimal Standard Model* (νMSM) [18, 19], a minimal extension of the SM by three RH neutrinos that aims to address several problems in particle physics and cosmology.[1] We use the νMSM as a standard example in what follows, but our results apply to any model that involves two sterile neutrinos with masses below the electroweak scale. Specific theoretical motivations for a low scale seesaw are *e.g.* based on classical scale invariance [22], the inverse seesaw framework [23, 24] and other models with an approximate conservation of lepton number (*e.g.* [25–35]).

In addition to the generation of light neutrino masses via the seesaw mechanism, RH neutrinos with masses below the electroweak scale could also generate the baryon asymmetry of the universe (BAU)[2] via low scale leptogenesis [37]. In contrast to thermal leptogenesis in scenarios with superheavy RH neutrinos [38], the BAU in these scenarios is not generated in the decay of the heavy neutrinos, but via CP violating oscillations during their production [37].

The minimal number n_s of RH neutrinos that is required to explain the two observed light neutrino mass differences is $n_s = 2$. This is the scenario on which we focus in the following. The same choice also effectively describes baryogenesis in the νMSM. Two of the three RH neutrinos in the νMSM generate the light neutrino masses and the BAU, while the third one is a Dark Matter (DM) candidate. The constraints on the mass and lifetime of the DM candidate imply that its mixing with ordinary neutrinos must be extremely tiny, see [39] and references therein, so that its effect on the magnitude of the light neutrino masses and the BAU is negligible. Hence, one can effectively describe the seesaw mechanism and baryogenesis in the νMSM by setting $n_s = 2$. An attractive feature of the νMSM is that it could in principle be an effective field theory up to the Planck scale [40], *i.e.* , all known phenomena in particle physics and cosmology may be explained without adding any new particles other than the RH neutrinos to the SM. From an experimental viewpoint this scenario is very attractive because the new particles (or traces of them) could be found in the laboratory [41, 42], and there is a realistic possibility of solving two of the most important puzzles in particle physics and cosmology.

The goal of this work is to derive constraints on the properties of the RH neutrinos from the requirement to simultaneously explain the light neutrino flavour oscillations and the BAU. If any heavy neutral leptons are discovered in future experiments, then it will be possible to use these constraints in order to assess whether these particles can indeed be the common origin of light neutrino masses and the baryonic matter in the universe. In the present analysis, we focus on the heavy neutrino mass range $100\,\mathrm{MeV} < M_i <$

[1] Detailed descriptions of the νMSM are *e.g.* given in Refs. [20, 21].

[2] A short review of the observational evidence for a matter-antimatter asymmetry in the observable universe and its theoretical implications is given in Ref. [36].

	m_1^2	m_2^2	m_3^2	$\sin^2\theta_{12}$	$\sin^2\theta_{13}$	$\sin^2\theta_{23}$
NO	0	$m_{\rm sol}^2$	Δm_{31}^2	0.308	0.0219	0.451
IO	$-\Delta m_{32}^2 - m_{\rm sol}^2$	$-\Delta m_{32}^2$	0	0.308	0.0219	0.576

Table 1: *Best fit values for the active neutrino masses m_i and mixings θ_{ij} for normal ordering (NO) in the top row and inverted ordering (IO) in the bottom row from Ref. [43]. The smaller measured mass difference, the so-called solar mass difference, is given by $m_{\rm sol}^2 = m_2^2 - m_1^2 = 7.49\times10^{-5}\,\text{eV}^2$. The larger mass differences are given by $\Delta m_{31}^2 = m_3^2 - m_1^2 = 2.477\times10^{-3}\,\text{eV}^2$ for NO and $\Delta m_{32}^2 = m_3^2 - m_2^2 = -2.465\times10^{-3}\,\text{eV}^2 < 0$ for IO. In case of $n_s = 2$ flavours we have $m_1 = 0$ for NO and $m_3 = 0$ for IO. The absolute value $|m_3^2 - m_1^2|$ is often referred to as the atmospheric mass difference $m_{\rm atm}^2$. Thus, for NO and $n_s = 2$ we have $m_{\rm atm}^2 = m_3^2$ and for IO $m_{\rm atm}^2 = m_1^2 = m_2^2 + \mathcal{O}(m_{\rm sol}^2/m_{\rm atm}^2)$. These values for $m_{\rm atm}^2$ differ slightly for the two hierarchies. However, the errors are of order $m_{\rm sol}^2/m_{\rm atm}^2$.*

40 GeV. In the context of the seesaw mechanism, masses below 100 MeV are disfavoured by cosmological constraints [10]. For masses larger than 40 GeV our treatment of leptogenesis in the early universe requires some refinements because the underlying assumption that the heavy neutrinos are fully relativistic while the BAU is generated is not justified.

This paper is organised as follows: In Section 2 we introduce the seesaw mechanism, define the active-sterile mixing and discuss the allowed parameter region that can be explained by neutrino oscillation data. Further constraints emerge by simultaneously imposing that the heavy neutrinos generate the experimentally observed BAU. The discussion of these constraints and corresponding plots are presented in Section 3. Future improvements of flavour predictions are listed in Section 4, and Appendix A summarises analytic expressions for the heavy neutrino mixing angles.

2 Testing the seesaw mechanism

The requirement to reproduce the observed properties of light neutrinos imposes considerable constraints on the heavy states N_i. If the splitting ΔM between the two heavy neutrino masses is too small to be experimentally resolved, which is the case in most of the leptogenesis parameter space, then the relative size of the couplings of the heavy neutrinos of a given mass to the three SM generations is fixed by the properties of the light neutrinos alone [44–46], *cf.* Eqs. (26,27,63,65) discussed below. These relations offer a powerful tool to test the seesaw mechanism as the origin of neutrino mass experimentally. With the exception of the Majorana phase, all light neutrino properties can be determined in the foreseeable future, leaving only one free parameter. If heavy neutral leptons are discovered experimentally and their couplings to all three SM generations are measured, these three observables overconstrain the part of the parameter space in the seesaw Lagrangian (1) that is related to the generation of light neutrino masses. Consistency with the relations derived in this Section would provide strong evidence that the discovered particle is indeed responsible for the seesaw mechanism of neutrino mass generation. In the subsequent Sections, we investigate which additional constraints can be derived from the requirement to explain the observed BAU and from other experiments.

2.1 The model parameters

The minimal type-I seesaw model is described by the Lagrangian

$$\mathcal{L} = \mathcal{L}_{\rm SM} + \frac{1}{2}\overline{\nu_{{\rm R}i}^c}(\mathrm{i}\partial\!\!\!/ - M)_{ij}\nu_{{\rm R}j} - Y_{ia}^*\overline{\ell_a}\varepsilon\phi\nu_{{\rm R}i} - Y_{ia}\overline{\nu_{{\rm R}i}}\phi^\dagger\varepsilon^\dagger\ell_a, \tag{1}$$

where $\mathcal{L}_{\rm SM}$ is the SM Lagrangian. The heavy neutrinos are represented by RH spinors $\nu_{{\rm R}i}$ and the superscript c denotes charge conjugation. They interact with the SM solely through their Yukawa interactions Y to the SM lepton doublets ℓ_a ($a = e, \mu, \tau$) and the Higgs field ϕ, where ε is the antisymmetric SU(2)-invariant tensor with $\varepsilon^{12} = 1$.

The connection between the Lagrangian (1) and low energy neutrino oscillation data is well known. Here we only recapitulate the main results that are required for the present analysis and refer the reader to Refs. [9, 13] for a recent summary. A convenient way to express the relation at tree level is provided by the Casas-Ibarra parametrisation [47][3]

$$Y^\dagger = \frac{\mathrm{i}}{v}U_\nu\sqrt{m_\nu^{\rm diag}}\mathcal{R}\sqrt{M^{\rm diag}}\,. \tag{2}$$

Here $(m_\nu^{\rm diag})_{ij} = \delta_{ij}m_i$ is the light neutrino mass matrix, and m_i are the light neutrino masses. Note that the number of non-vanishing eigenvalues m_i cannot be larger than n_s. This immediately implies that the lightest neutrino is massless in the scenario with $n_s = 2$ we consider here ($m_{\rm lightest} = 0$).[4] The light neutrino mixing matrix V_ν can be expressed as $V_\nu = (\mathbb{1} - \frac{1}{2}\theta\theta^\dagger)U_\nu$, where the unitary matrix U_ν diagonalises the matrix

$$m_\nu = v^2 Y^\dagger M^{-1} Y^* \tag{3}$$

and can be factorised as

$$U_\nu = V^{(23)}U_\delta V^{(13)}U_{-\delta}V^{(12)}\mathrm{diag}(e^{\mathrm{i}\alpha_1/2}, e^{\mathrm{i}\alpha_2/2}, 1)\,, \tag{4}$$

with $U_{\pm\delta} = \mathrm{diag}(1, e^{\mp\mathrm{i}\delta/2}, e^{\pm\mathrm{i}\delta/2})$.
The non-vanishing entries of the matrix $V = V^{(23)}V^{(13)}V^{(12)}$ are given by

$$V_{ii}^{(ij)} = V_{jj}^{(ij)} = \cos\theta_{ij}\ ,\ V_{ij}^{(ij)} = -V_{ji}^{(ij)} = \sin\theta_{ij}\ ,\ V_{kk}^{(ij)} = 1 \quad \text{for } k \neq i, j\,. \tag{5}$$

The parameters θ_{ij} are the the mixing angles of the light neutrinos, δ is referred to as the Dirac phase and $\alpha_{1,2}$ as Majorana phases. Only one combination of the Majorana phases is physical for $n_s = 2$. For normal hierarchy this is α_2, for inverted hierarchy it is $\alpha_1 - \alpha_2$. The deviation of V_ν from unity is due to the mixing between the doublet states $\nu_{\rm L}$ and the singlet state $\nu_{\rm R}$. It is quantified by the parameters

$$\theta = vY^\dagger M^{-1}\,. \tag{6}$$

[3]The relation (2) between Y and the light neutrino properties holds at tree level and at leading order in the parameters θ_{ai} defined below. A generalisation that holds at one loop level has been introduced in Ref. [48]. However, the results found in Ref. [49] suggest that the tree level treatment is sufficient in the parameter region where leptogenesis is viable.

[4]This statement practically also applies to the νMSM because the coupling of the third RH neutrino is so feeble that its contribution to the generation of light neutrino masses can be neglected.

Here v is the temperature dependent Higgs expectation value with $v = 174\,\mathrm{GeV}$ at temperature $T = 0$. The complex orthogonal matrix $\mathcal{R}$ fulfils the condition $\mathcal{R}\mathcal{R}^T = 1$ and can be expressed as

$$\mathcal{R}^{\rm NO} = \begin{pmatrix} 0 & 0 \\ \cos\omega & \sin\omega \\ -\xi\sin\omega & \xi\cos\omega \end{pmatrix}, \qquad \mathcal{R}^{\rm IO} = \begin{pmatrix} \cos\omega & \sin\omega \\ -\xi\sin\omega & \xi\cos\omega \\ 0 & 0 \end{pmatrix}, \tag{7}$$

where $\xi = \pm 1$ and $\omega = \mathrm{Re}\omega + \mathrm{iIm}\omega$ is the complex mixing angle. For large $|\mathrm{Im}\omega| \gg 1$ one obtains the useful expansion

$$\mathcal{R}^{\rm NO}_{|\mathrm{Im}\omega|\gg 1} = \frac{1}{2} e^{\mathrm{Im}\omega} e^{-\mathrm{iRe}\omega} \begin{pmatrix} 0 & 0 \\ 1 & \mathrm{i} \\ -\xi\mathrm{i} & \xi \end{pmatrix}, \qquad \mathcal{R}^{\rm IO}_{|\mathrm{Im}\omega|\gg 1} = \frac{1}{2} e^{\mathrm{Im}\omega} e^{-\mathrm{iRe}\omega} \begin{pmatrix} 1 & \mathrm{i} \\ -\xi\mathrm{i} & \xi \\ 0 & 0 \end{pmatrix}. \tag{8}$$

To second order in $|\theta_{ai}| \ll 1$, the three light neutrino mass eigenstates with masses m_i can be expressed in terms of the Majorana spinors

$$\nu_i = \left[V_\nu^\dagger \nu_{\rm L} - U_\nu^\dagger \theta \nu_{\rm R}^c + V_\nu^T \nu_{\rm L}^c - U_\nu^T \theta \nu_{\rm R} \right]_i . \tag{9}$$

In addition, there are n_s heavy mass eigenstates

$$N_i = \left[V_N^\dagger \nu_{\rm R} + \Theta^T \nu_{\rm L}^c + V_N^T \nu_{\rm R}^c + \Theta^\dagger \nu_{\rm L} \right]_i . \tag{10}$$

The unitary matrix U_N diagonalises the heavy neutrino mass matrix

$$M_N = M + \frac{1}{2}(\theta^\dagger \theta M + M^T \theta^T \theta^*) , \tag{11}$$

and $V_N = (1 - \frac{1}{2}\theta^T\theta^*)U_N$. We shall refer to the basis where M_N is diagonal as the *mass basis* of the heavy neutrinos, while the basis where $Y^\dagger Y$ is diagonal is the *interaction basis*. The *mass states* are the eigenstates of $M_N^\dagger M_N$, with physical mass squares given by the eigenvalues of that matrix. The *interaction states* are the eigenstates of $YY^\dagger$, their interaction strengths are characterised by the eigenvalues of that matrix.[5]

An experimental confirmation of the seesaw mechanism requires the discovery of the new particles N_i. They interact with ordinary matter via their quantum mechanical mixing. If kinematically allowed, they appear in any process that involves ordinary neutrinos, but with an amplitude that is suppressed by the "mixing angle"

$$\Theta_{ai} = (\theta U_N^*)_{ai} \approx \theta_{ai} \ . \tag{12}$$

Hence, the branching ratios can be expressed in terms of the quantities

$$U_{ai}^2 = |\Theta_{ai}|^2 \approx |\theta_{ai}|^2 . \tag{13}$$

[5]That statement has to be taken with some care because the interactions are in principle helicity dependent.

It is a main goal of this work to make predictions about the flavour mixing pattern of the heavy neutrinos, *i.e.* the relative size of the U_{ai}^2 for the different $a = e, \mu, \tau$. Leptogenesis with $n_s = 2$ is known to require a mass degeneracy $|\Delta M| \ll \bar{M}$, where

$$\bar{M} = \frac{M_2 + M_1}{2} \; , \; \Delta M = \frac{M_2 - M_1}{2} \, . \tag{14}$$

If the mass splitting ΔM is too small to be resolved experimentally, then experimental constraints should be applied to the quantities

$$U_a^2 = \sum_i U_{ai}^2 \, . \tag{15}$$

Finally, the overall coupling strength of the heavy neutrinos can be quantified by

$$U^2 = \sum_a U_a^2 \, . \tag{16}$$

In terms of the Casas-Ibarra parameters, U^2 reads

$$U^2 \;\; = \;\; \frac{M_2 - M_1}{2M_1 M_2} (m_2 - m_3) \cos(2\mathrm{Re}\omega) + \frac{M_1 + M_2}{2M_1 M_2} (m_2 + m_3) \cosh(2\mathrm{Im}\omega) \tag{17}$$

with normal hierarchy and

$$U^2 \;\; = \;\; \frac{M_2 - M_1}{2M_1 M_2} (m_1 - m_2) \cos(2\mathrm{Re}\omega) + \frac{M_1 + M_2}{2M_1 M_2} (m_1 + m_2) \cosh(2\mathrm{Im}\omega) \tag{18}$$

with inverted hierarchy. For given mass spectrum, the magnitude of U^2 is determined by ω alone.

2.2 Constraints from neutrino oscillation data

If there are no cancellations in the light neutrino mass matrix m_ν, then one expects all U^2 to be of the order of the *naive seesaw expectation*

$$U^2 \sim \sqrt{m_{\rm atm}^2 + m_{\rm lightest}^2} / \bar{M} \, . \tag{19}$$

Mixing angles much larger than the estimate (19) can only be made consistent with small neutrino masses and non-observation of neutrinoless double β ($0\nu\beta\beta$) decay if there are cancellations that keep the eigenvalues of m_ν small in spite of comparably large Yukawa couplings [13, 48]. Such cancellations are *e.g.* expected in models with an approximate conservation of $B - L$. If $B - L$ were an exact symmetry of the Lagrangian (1), the heavy neutrino mass eigenstates N_i would have exactly the same mass $\bar{M}$ and couplings

$$U_{a1}^2 = U_{a2}^2 = U_a^2/2 \, , \tag{20}$$

and they could be combined into a Dirac spinor

$$\Psi_N = \frac{1}{\sqrt{2}}(N_1 + \mathrm{i}N_2)\,. \tag{21}$$

While this limit cannot be realised within the seesaw approximation with $m_i \neq 0$, it can be reached approximately in the limit $\Delta M \to 0$, $|\mathrm{Im}\omega| \to \infty$. In this limit, inserting Eq. (8) into the parametrisation (2) yields $Y_{a2}^\dagger = \mathrm{i}Y_{a1}^\dagger$. The equality (20) can then be obtained by making use of Eq. (13). In the experimentally most accessible region we can therefore expand in the small $B - L$ violating parameters

$$\mu = \Delta M/\bar{M}\ ,\ \epsilon = e^{-2\mathrm{Im}\omega}\,. \tag{22}$$

In the limit $\mu = 0$ and $\epsilon \to 0$, one finds

$$\theta_{a2} \simeq \mathrm{i}\theta_{a1} \tag{23}$$

and the interaction eigenstates approximately become

$$N_\mathrm{s} \simeq \frac{1}{\sqrt{2}}(N_1 + iN_2) = \Psi_N\ ,\ N_\mathrm{w} \simeq \frac{1}{\sqrt{2}}(N_1 - iN_2) = \Psi_N^c. \tag{24}$$

The interactions of N_w are of order ϵ, while those of N_s scale as $1/\epsilon$. More precisely, the larger eigenvalue of $YY^\dagger$ scales as $[(m_i - m_j)\bar{M}]/(4v^2\epsilon)$, where m_i and m_j are the two non-zero light neutrino masses. As usual, only the right chiral part of the spinors N_s and N_w interacts with the SM.

This argument can be generalised to the case $n_s > 2$, where leptogenesis does not require a mass degeneracy [50]; mixings much larger than (19) always require that the heavy neutrino mass spectrum is organised in pairs of particles with quasi-degenerate masses. This has important phenomenological implications. Searches for lepton number violating processes are often considered to be the golden channel to look for heavy Majorana neutrinos. However, in the context of the seesaw mechanism, these processes are suppressed by small parameters μ and ϵ if U^2 is much larger than suggested by (19). Hence, the bounds published by experimental collaborations cannot be directly applied to the seesaw partners N_i if they are based on searches for LNV.

The Dirac phase δ is expected to be measured in the next generation of neutrino oscillation experiments. If heavy neutral leptons are found experimentally and their mass spectrum can be resolved, then independent measurements of all six U_{ai}^2, which is *e.g.* possible at SHiP [51, 52], would not only allow to reconstruct all unknown parameters, but even to overconstrain the system. Additional cross-checks are provided by indirect searches for the traces of RH neutrinos, such as $0\nu\beta\beta$ decay. This would be a very powerful test to assess whether these heavy neutral leptons indeed generate the light neutrino masses via the seesaw mechanism. Moreover, the BAU generated by these heavy neutrinos could be calculated from measured quantities and compared to the observed value, leading to a fully testable leptogenesis scenario [46]. However, most realistic experiments are only sensitive

to values of U^2 much larger than the naive seesaw relation (19). Consistency with neutrino oscillation data and non-observation of $0\nu\beta\beta$ decay requires $\mu, \epsilon \ll 1$ in this region. While this leads to convenient simplifications, it also implies a loss of sensitivity to the parameters ΔM and Reω, *cf.* Eqs. (17) and (18). These are however crucial in determining the BAU generated via leptogenesis. Therefore, the remaining Sections of this paper, in particular Sections 3 and 4, are devoted to study the perspectives of testing the seesaw mechanism and leptogenesis in the limit $\mu, \epsilon \ll 1$.

In the following we set $\mu = 0$ and only keep terms of order $1/\epsilon$. Just for illustrative purposes, we now further expand in $m_{\rm sol}/m_{\rm atm}$ and find that

$$U^2 \simeq \frac{1}{2\bar{M}} m_{\rm atm} e^{2{\rm Im}\omega} \text{ for NO}\,, \tag{25a}$$

$$U^2 \simeq \frac{1}{\bar{M}} m_{\rm atm} e^{2{\rm Im}\omega} \text{ for IO}\,, \tag{25b}$$

where we have assumed ${\rm Im}\omega > 0$. Hence, the overall interaction strength of the N_i in this approximation is fixed by the parameters $\bar{M}$, Imω and $m_{\rm atm}$ alone. For normal hierarchy we furthermore obtain

$$U_e^2 \approx e^{2{\rm Im}\omega} \frac{m_{\rm atm}}{2\bar{M}} \sin^2\theta_{13}\,, \tag{26a}$$

$$U_\mu^2 \approx e^{2{\rm Im}\omega} \frac{m_{\rm atm}}{2\bar{M}} \cos^2\theta_{13} \sin^2\theta_{23}\,, \tag{26b}$$

$$U_\tau^2 \approx e^{2{\rm Im}\omega} \frac{m_{\rm atm}}{2\bar{M}} \cos^2\theta_{13} \cos^2\theta_{23}\,. \tag{26c}$$

Since $\bar{M}$ can be determined kinematically, Imω is the only free parameter, and the system of Eqs. (26) is overconstrained. A measurement of any of the U_a^2 already determines Imω in this approximation. The main prediction of Eqs. (26) is that U_e^2 is suppressed with respect to U_μ^2 and U_τ^2 due to the relative smallness of θ_{13}. On the other hand, U_μ^2 and U_τ^2 are expected to be comparable in size because $\theta_{23} \simeq \pi/4$. For inverted hierarchy we neglect θ_{13} and $\theta_{23} - \pi/4$ in order to obtain simple relations:

$$U_e^2 \approx e^{2{\rm Im}\omega} \frac{m_{\rm atm}}{2\bar{M}} \left[1 + \xi \sin\left(\frac{\alpha_2 - \alpha_1}{2}\right) \sin(2\theta_{12})\right], \tag{27a}$$

$$U_\mu^2 \approx e^{2{\rm Im}\omega} \frac{m_{\rm atm}}{4\bar{M}} \left[1 - \xi \sin\left(\frac{\alpha_2 - \alpha_1}{2}\right) \sin(2\theta_{12})\right], \tag{27b}$$

$$U_\tau^2 \approx U_\mu^2\,. \tag{27c}$$

The results from Eqs. (25)-(27) are consistent with previous results from Ref. [46] as well as the more detailed expressions in Appendix A. In the approximation above, observing U_e^2 and U_μ^2 would not only allow to measure Imω, but also the Majorana phase difference $\alpha_2 - \alpha_1$. Note that the relevant observables for inverted hierarchy only depend on the Majorana phase difference $\alpha_2 - \alpha_1$, which is the only physical combination. An additional measurement of U_τ^2 would again overconstrain the system of Eqs. (27).

The relations (26) and (27) are quite useful to get a rough understanding of the parametric dependencies and, further, they allow to identify which parameters would be most strongly constrained by measurements of the U_a^2. At a quantitative level, the quantities $\theta_{23} - \pi/4$, θ_{13} and $m_{\rm sol}/m_{\rm atm}$ are not small enough to be neglected,[6] and the dependence of the U_a^2 on the phases δ, α_1 and α_2 has to be taken into account. The full expressions in the limit $\mu, \epsilon \ll 1$ are given in Appendix A. Figure 1 shows the range of U_a^2/U^2 that can be realised by varying the phases. Figure 11 illustrates the dependence of U_a^2/U^2 on the phases.

2.3 Other constraints

Direct searches for heavy neutrinos in fixed target experiments and colliders impose upper bounds on the U_{ai}^2 for given M_i. The properties of heavy neutrinos are constrained indirectly by searches for rare processes and precision observables, which can be affected by their existence. Various collections of constraints have been presented in Refs. [7, 9–15, 53–56]. In order to identify the range of U_a^2 that is consistent with the constraints from past experiments for given $\bar{M}$, we perform a numerical scan of parameter space. We fix all light neutrino parameters to their best fit values, set $\alpha_1 = 0$ and $\xi = 1$. We then randomise all other parameters, using flat priors for δ, α_2, Reω and Imω and a logarithmic prior for ΔM. We restrict ΔM to values less than 10 MeV, which roughly corresponds to the largest mass splitting found to be consistent with leptogenesis for $n_s = 2$ in Ref. [21].[7] This means that the experiments under consideration could not resolve N_1 and N_2 kinematically, and constraints apply to U_a^2 (rather than the individual U_{ai}^2). From a sample of 10^7 randomly generated sets of parameters we identify the largest and smallest U_a^2 for fixed values $\bar{M}$ between the pion and W boson mass that are consistent with the negative results of past direct and indirect searches. We take into account constraints from the direct search experiments DELPHI [57], L3 [58], LHCb [59], ATLAS [60], CMS [61], BELLE [62], BEBC [63], FMMF [64], E949 [65], PIENU [66], NOMAD [67], TINA [68], PS191 [69], CHARM [70, 71], CHARMII [72], NuTeV [73], NA3 [74] and kaon decays [75, 76]. For peak searches below the kaon mass, we use the summary given in [7], and for PS191 we use the reinterpretation given in [45]. We combine these with indirect constraints from searches for $0\nu\beta\beta$ decays [77, 78], lepton universality [79–81], violation of CKM unitarity [11, 81–85], LNV decays [86, 87] and with electroweak precision data [88–91]. In order to remain consistent with neutrino oscillation data even for large values of Imω, we use the radiatively corrected Casas Ibarra parametrisation introduced in Ref. [48] instead of Eq. (2) for the purpose of the scan. Finally, we impose the constraint that the N_i lifetime is shorter than 0.1 s, based on the various decay rates given in Refs. [21, 92]. This requirement is motivated by the fact that the heavy neutrinos, which come into thermal equilibrium in the

[6] Note that the leading order correction in $m_{\rm sol}$ is of order $\sqrt{m_{\rm sol}/m_{\rm atm}} \sim 1/2$, which is not a good expansion parameter.

[7] More recent studies [46, 49] suggest that there exists a small part of the parameter space where leptogenesis is possible with slightly larger ΔM. For $n_s = 3$ leptogenesis does not require a mass degeneracy [50].

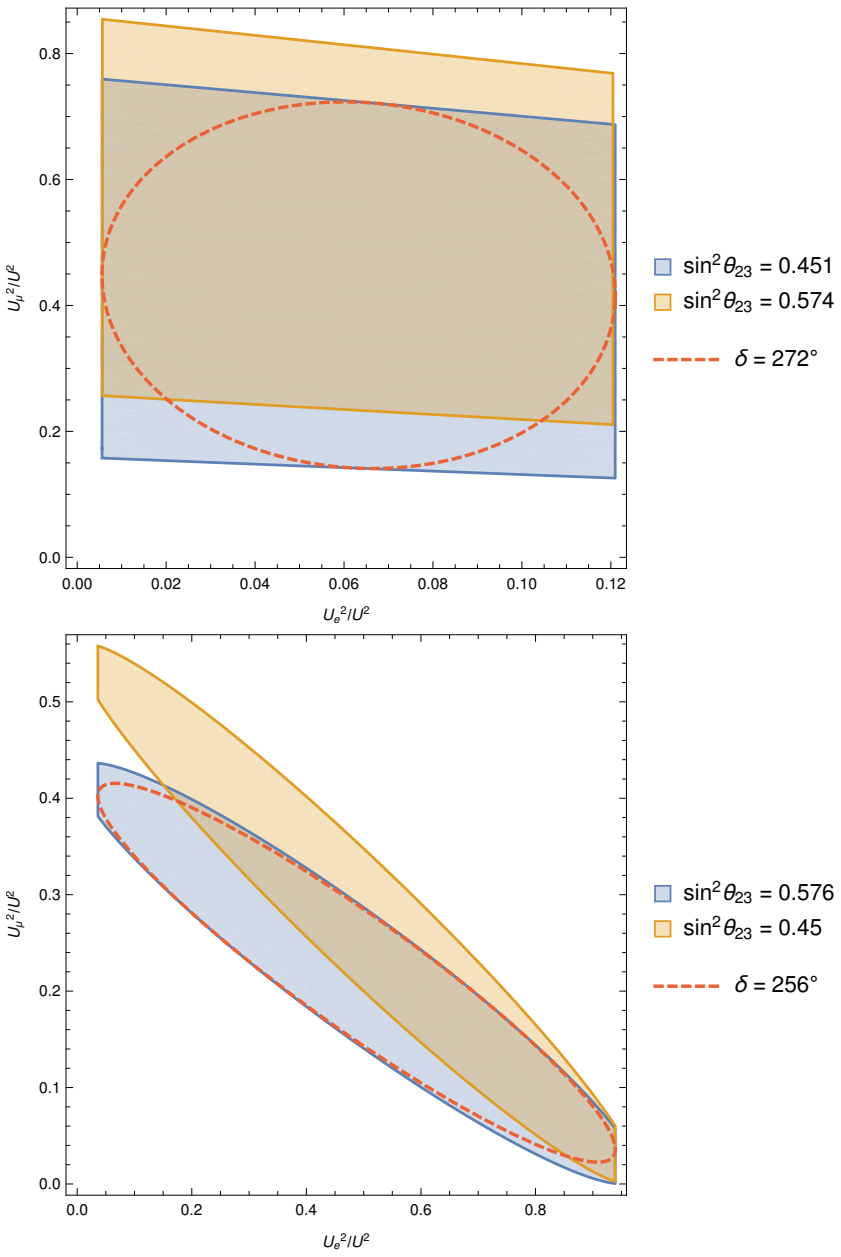

Figure 1: *The coloured regions indicate the allowed range of* U_a^2/U^2 *that can be realised by varying the phases in* U_ν *after fixing the light neutrino mass splittings and mixing angles to their best fit values given in Table 1.* U_τ^2/U^2 *is fixed by the requirement* $\sum_a U_a^2/U^2 = 1$*. The difference between the orange and blue region illustrates the change of the predictions if one varies these parameters within their experimental uncertainties. The upper panel assumes normal light neutrino mass hierarchy, the lower panel assumes inverted hierarchy. If the Dirac phase* δ *is measured independently in light neutrino oscillation experiments, the two dimensional regions will reduce to rings in the* U_e^2/U^2*-*U_μ^2/U^2 *plane as demonstrated by the red dashed lines, where we take the best fit values for* $\delta = 272°$ *for normal hierarchy with* $\sin^2\theta_{23} = 0.451$ *and* $\delta = 256°$ *with* $\sin^2\theta_{23} = 0.576$ *for inverted hierarchy.*

early universe [93], should have decayed before the formation of light elements in big bang nucleosynthesis (BBN) [94]. The precise implementation of all these conditions is discussed in detail in Ref. [13]. The results are shown in Figures 2-3. Potential future improvements are discussed in Section 4. We find that indirect search constraints other than neutrino oscillation data do not significantly affect the range of the allowed U_a^2. This is consistent with what has previously been found in Refs. [12, 95]. However, the interplay between direct search bounds, neutrino oscillation data and BBN leads to non trivial combined constraints that are much stronger than one would expect from superimposing the regions excluded by each of these individually in the $\bar{M} - U_a^2$ plane.

2.3.1 Normal hierarchy

Mixing U_e^2 with electron flavour – The constraints on U_e^2 for normal hierarchy are shown in the upper panel of Figure 2. For $\bar{M}$ below the kaon mass m_K, the global constraints are much stronger than the direct search constraints alone. The reason is the interplay between the direct search bounds on U_e^2 and U_μ^2, neutrino oscillation data and the lower bound on U_a^2 from BBN. The latter requires at least one of the U_a^2 to be sufficiently large that the heavy neutrinos decay in less than 0.1s. In order to make this consistent with very small U_e^2, either U_μ^2 or U_τ^2 have to be sizeable. The direct search constraint on U_τ^2 is rather weak, but neutrino oscillation data does not allow U_τ^2 to be larger than U_μ^2 by more than a factor $\sim 5 - 6$, see Figure 1. Hence, the rather strong bounds on U_μ^2 from the experiments PS191 and E494 also forbids large values of U_τ^2. In combination, this implies that U_e^2 must not be too small in order to be consistent with BBN, and a significant fraction of the heavy neutrino mass region below $\bar{M} = m_K$ is in fact already ruled out. This is clearly visible by looking and the constraints on U_μ^2 in the middle panel of Figure 2. This is not obvious if one simply superimposes the upper bound on U_e^2 from direct searches and the lower bound from BBN, which are separated by an order of magnitude for $\bar{M}$ near the kaon mass. The lower bound is dominated by BBN for masses below ~ 1 GeV. For larger masses it is determined by the requirement that at least one of the N_i must mix with electron flavour in order explain the observed light neutrino oscillation data. This constraint is sometimes called the *seesaw constraint*. It does not apply to individual U_{ai}^2, but does impose a lower bound on all U_a^2.

For $\bar{M}$ between the kaon and D meson mass m_D, the combined constraints on U_e^2 are essentially identical with the stronger one amongst the direct search constraints on U_e^2 and U_μ^2. The reason why the direct search constraint on U_μ^2 effectively also acts as an upper bound on U_e^2 is that, for normal hierarchy, U_e^2 must be smaller than U_μ^2 to be consistent with neutrino oscillation data, see Figure 1. There is only a small region slightly above m_D in which the combined constraints are much stronger than the direct constraint on any of the U_a^2. This has already been pointed out in Ref. [13]. It is related to the fact that the CHARM experiment imposes constraints on combinations of the U_a^2 [45].

For all other masses between m_D and the W boson mass m_W, the global constraint can be understood as a combination of the direct search bound from the DELPHI experiment at LEP and neutrino oscillation data. The shape of the upper bound on U_e^2 as a function

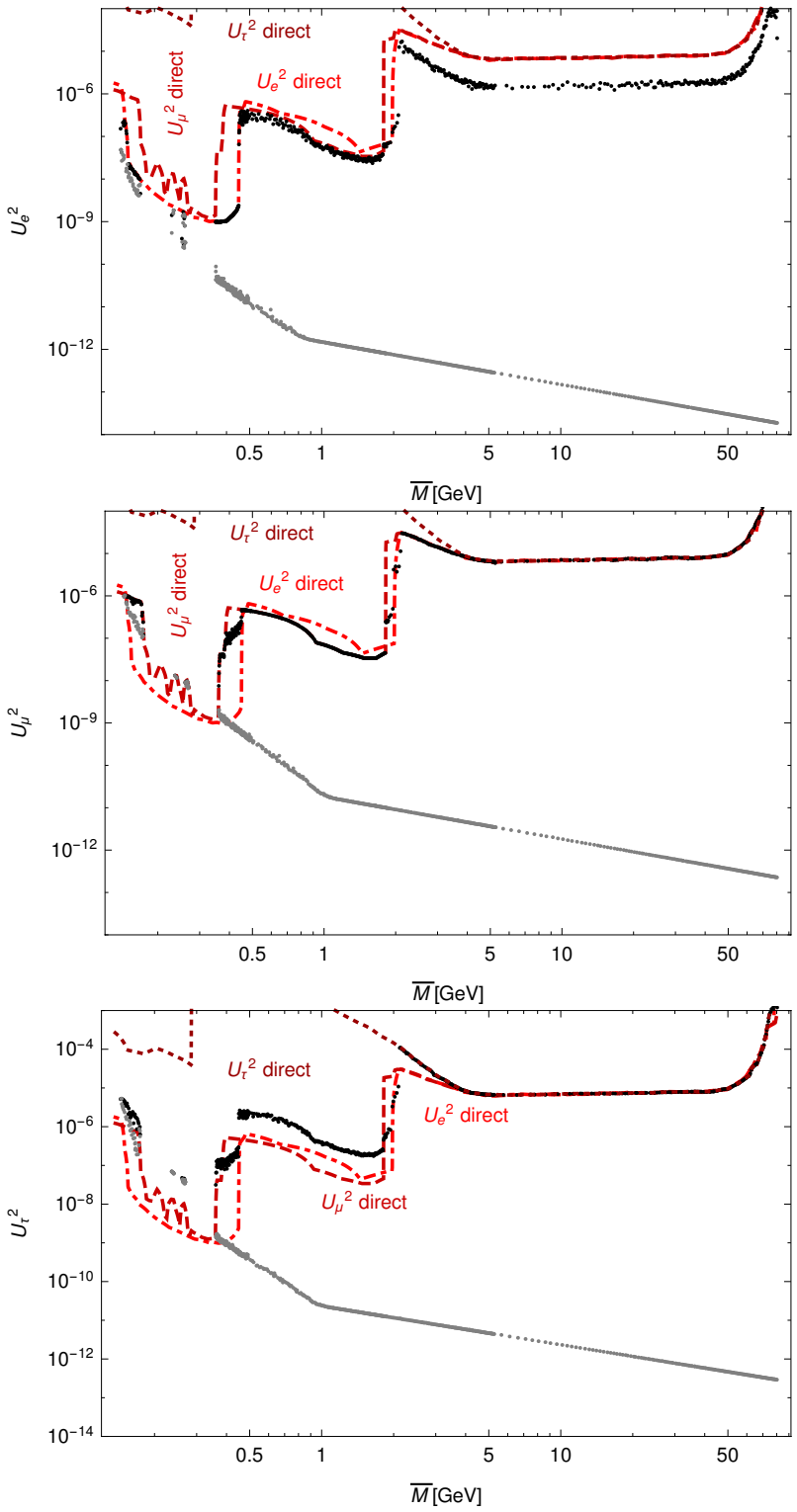

Figure 2: *Global constraints from direct and indirect search experiments and BBN for normal hierarchy and $\Delta M < 10$ MeV. The black and grey dots mark the largest and smallest value of U_a^2 we found to be consistent with all constraints in each mass bin. For comparison, the red lines show the direct search constraints from collider and fixed target experiments on U_e^2 (dashed-dotted), U_μ^2 (dashed) and U_τ^2 (dotted) alone.*

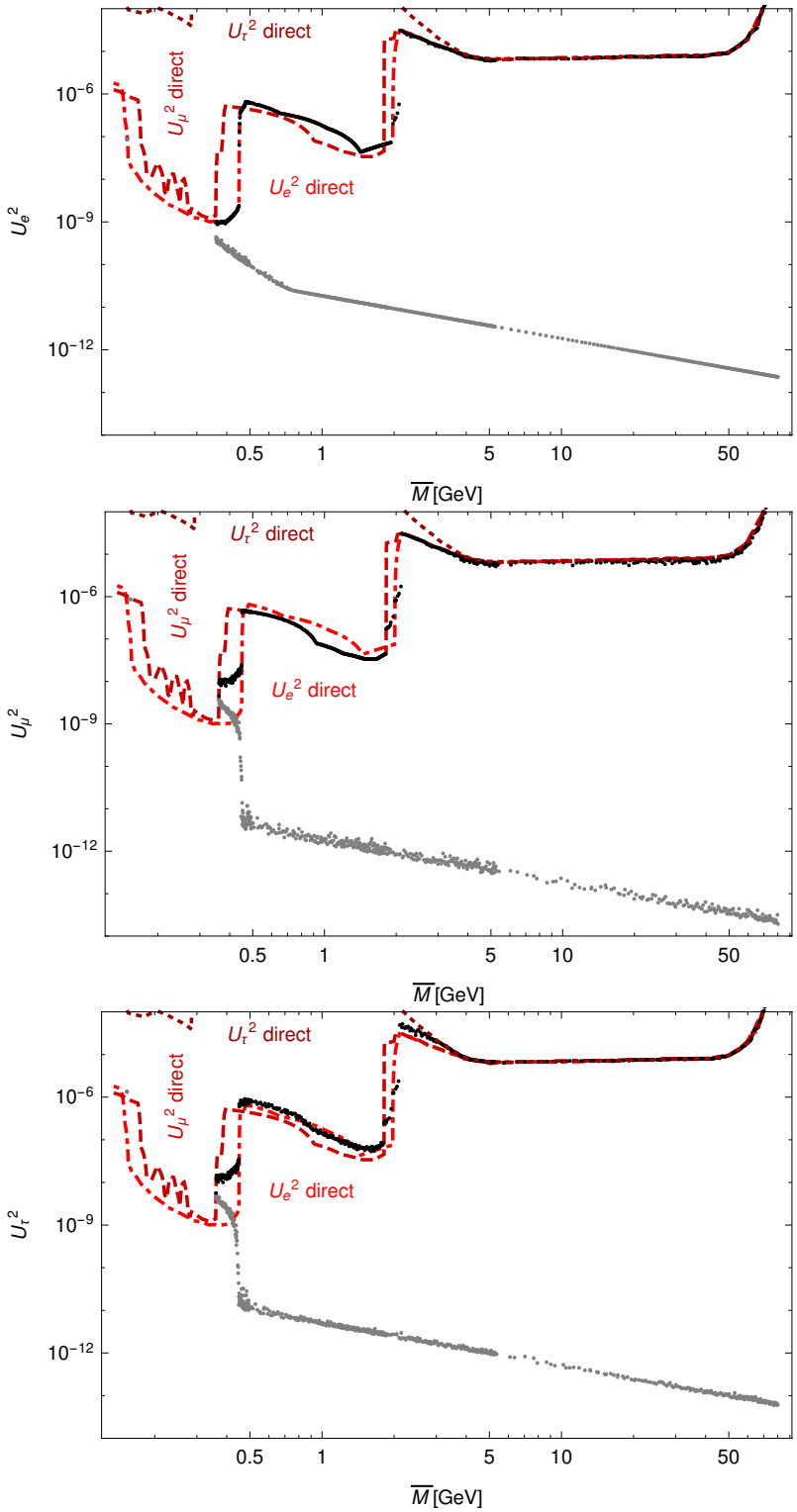

Figure 3: *Global constraints from direct and indirect search experiments and BBN for inverted hierarchy and $\Delta M < 10$ MeV. The black and grey dots mark the largest and smallest value of U_a^2 we found to be consistent with all constraints in each mass bin. For comparison, the red lines show the direct search constraints from collider and fixed target experiments on U_e^2 (dashed-dotted), U_μ^2 (dashed) and U_τ^2 (dotted) alone.*

of $\bar{M}$ is determined by the DELPHI bound, which is more or less the same for all U_a^2. However, since neutrino oscillation data requires U_e^2 to be an order of magnitude smaller than $U_\mu^2 + U_\tau^2$, the combined constraint on U_e^2 is about a factor 5 stronger than the direct search bound and is saturated when $U_\mu^2 \simeq U_\tau^2$.

Mixing U_μ^2 with muon flavour – As already explained in the for U_e^2, significant fractions of the region $\bar{M} < m_K$ are excluded by the interplay of direct search constraints, neutrino oscillation data and BBN. For almost all values above m_K, the combined bound is identical with the direct search bound alone. This is easy to understand: Constraints on U_e^2 have almost no effect on the combined constraint on U_μ^2 because neutrino oscillation data in any case implies $U_e^2 < U_\mu^2$, and constraints on U_τ^2 are never stronger than those on U_μ^2. The only exception is the small region near m_D already mentioned in the discussion on U_e^2.

Mixing U_τ^2 with tauon flavour – The direct search constraints on U_τ^2 for $\bar{M}$ below m_D are much weaker than those on U_e^2 and U_μ^2. As a result, the combined constraint on U_τ^2 is much stronger than the direct search constraint. As mentioned above, the strong constraints on U_μ^2 and U_e^2 rule out some part of the region $\bar{M} < m_D$. In the allowed mass region below m_D, the combined bound on U_τ^2 tracks the direct search constraint on U_e^2, but is weaker by the amount that neutrino oscillation data allows U_τ^2 to exceed U_e^2 (about two orders of magnitude if U_μ^2 takes the smallest allowed value). For $m_K < \bar{M} < m_D$ it tracks the direct search bound on U_μ^2 in the same way, but the factor by which U_τ^2 can exceed U_μ^2 is smaller (roughly a factor 5, see Figure 1). For masses $\bar{M} > m_D$, the combined constraint essentially equals the direct search constraint from DELPHI.

2.3.2 Inverted hierarchy

Mixing U_e^2 with electron flavour – For inverted hierarchy, most of the mass region $\bar{M} < m_K$ is excluded.

Mixing U_μ^2 with muon flavour – The combined lower bound on U_μ^2 for $\bar{M} < m_K$ is much stronger than that from BBN or the seesaw constraint alone. The reason is that a small U_μ^2 for inverted hierarchy necessarily comes at the price of a comparably large U_e^2, see Figure 1. This leads to a conflict with the upper bound on U_e^2 from the PS191 experiment even for values of U_μ^2 that are two orders of magnitude larger than the lower bound from BBN and/or the seesaw constraint. As a result, almost the entire mass region below ~ 350 MeV is ruled out, as this combined lower bound is in conflict with the upper bound from the PS191 experiment.

For $\bar{M} > m_K$, the combined upper bound on U_μ^2 equals the direct search bound in almost the entire mass range we consider, with the exception of the small region above m_D that also exists for normal hierarchy (*cf.* Section 2.3.1). The lower bound is given by the seesaw constraint.

Mixing U_τ^2 with tauon flavour –

For $\bar{M}$ below m_K, the situation for U_τ^2 is essentially the same as for U_μ^2. In the regime $m_K < \bar{M} < m_D$, the combined upper bound tracks the direct search bound on U_μ^2, but is slightly weaker because neutrino oscillation data permits U_τ^2 to be slightly larger than U_μ^2. For masses $\bar{M} > m_D$, the combined constraint essentially equals the direct search constraint from DELPHI. The lower bound is given by the seesaw constraint.

2.4 Higgs contribution to heavy neutrino masses

Eq. (11) implies that the neutrino mass matrix has an $\mathcal{O}(\theta^2)$ contribution from the coupling to the Higgs field. This contribution is crucial in the νMSM because it allows to adjust the physical mass splitting in a way that the asymmetry production is resonantly enhanced during both, the N_i production at $T > T_{\rm sph}$ and the N_i decay at $T \ll T_{\rm sph}$ [96]. The latter is needed for resonant SM production [97] via the Shi-Fuller mechanism [98]. This adjustment imposes a constraint on the parameter Reω [21]. The role of the $\mathcal{O}(\theta^2)$ term in Eq. (11) has largely been neglected in studies that address the behaviour of N_i in the laboratory. Before moving on to discuss cosmological bounds, we point out that it may be relevant for the interpretation of experimental data in the pseudo-Dirac regime $\epsilon, \mu \ll 1$ and affect some of the future analyses proposed in Section 4. By neglecting terms of $\mathcal{O}(\mu\, m_i)$, one can approximate the mass of the right-handed neutrinos by

$$
\begin{aligned}
M_N &= M + v^2 \mathrm{Re}[YY^\dagger]/\bar{M} \\
&= \begin{cases}
M + \frac{m_2+m_3}{2}\cosh(\mathrm{Im}\omega) + \frac{m_2-m_3}{2}\begin{pmatrix} \cos 2\mathrm{Re}\omega & \sin 2\mathrm{Re}\omega \\ \sin 2\mathrm{Re}\omega & -\cos 2\mathrm{Re}\omega \end{pmatrix} & \text{for NO,} \\
M + \frac{m_1+m_2}{2}\cosh(\mathrm{Im}\omega) + \frac{m_1-m_2}{2}\begin{pmatrix} \cos 2\mathrm{Re}\omega & \sin 2\mathrm{Re}\omega \\ \sin 2\mathrm{Re}\omega & -\cos 2\mathrm{Re}\omega \end{pmatrix} & \text{for IO.}
\end{cases}
\end{aligned}
\tag{28}
$$

For $\epsilon, \mu \ll 1$, the contribution to the difference between the eigenvalues of M_N from the coupling to the Higgs field can be estimated as

$$
\Delta M_{\theta\theta} \approx \begin{cases} m_2 - m_3 \approx 4.11 \times 10^{-11}\,\mathrm{GeV} & \text{for NO,} \\ m_1 - m_2 \approx 7.60 \times 10^{-13}\,\mathrm{GeV} & \text{for IO.} \end{cases}
\tag{29}
$$

As a consequence, the physical mass splitting cannot be smaller than the light neutrino mass splitting $\Delta m_{\rm atm}$ unless the parameters are specifically chosen such that there are cancellations between the term involving the mass splitting in M and the $\mathcal{O}(\theta^2)$ term in M_N. In such a situation, also radiative corrections to the mass splitting have to be considered [99]. Furthermore, the inclusion of the θ^2 term can change the alignment between the interaction and mass bases: For $\Delta M \lesssim \Delta M_{\theta\theta}$, the mass basis is effectively identical to the interaction basis. As a result, for $\Delta M \lesssim \Delta M_{\theta\theta}$ the calculations of the CP violation [100, 101], discussions about the oscillations in the detector [102, 103] and work on distinguishing the Dirac and Majorana nature of the right-handed neutrinos from collider signatures [104–106] may need to be revisited.

3 Constraints from leptogenesis

In the previous Section we have seen that the requirement to explain the observed light neutrino masses via the seesaw mechanism already imposes considerable constraints on the mass spectrum and flavour mixing pattern of heavy neutrinos with observably large U^2. In this Section we explore which additional constraints can be obtained from the requirement to explain the observed BAU.

3.1 Leptogenesis from neutrino oscillations

The basic idea behind leptogenesis is that a matter-antimatter asymmetry is generated in the lepton sector and then partly transferred into a baryon number by weak sphaleron processes [107] that violate $B + L$ and conserve $B - L$. B is conserved at temperatures T below the temperature $T_{\rm sph} \simeq 130\,{\rm GeV}$ [108] of sphaleron freezeout, so that the BAU is determined by the lepton asymmetry L at $T = T_{\rm sph}$. Traditionally it is assumed that $\bar{M}$ is much larger than the electroweak scale. In this case, the N_i become Maxwell suppressed long before sphaleron freezeout, and the BAU is generated by their CP violating decay [38]. For $\bar{M}$ below the electroweak scale, the seesaw relation (3) implies that the Yukawa couplings must be rather small, and the N_i production in the early universe is so slow that they may not reach thermal equilibrium before $T = T_{\rm sph}$.[8] Then the BAU is generated via CP violating flavour oscillations amongst the N_i during their production [37].We do not repeat the detailed description of this mechanism here, which has been studied by various authors [18, 21, 22, 37, 46, 49, 50, 96, 109–122]. Depending on the model parameters, one can identify two qualitatively different ranges of dynamic behaviour that we refer to as the *oscillatory regime* and the *overdamped regime* [121]. These are distinguished by the hierarchy between the heavy neutrino oscillation frequency and the rates at which the heavy neutrino interaction eigenstates approach thermal equilibrium in the symmetric phase of the SM, which are given by the eigenvalues of the matrix $\Gamma_N \simeq YY^\dagger \gamma_{\rm av} T$. Here $\gamma_{\rm av}$ is a numerical coefficient which we set to $\gamma_{\rm av} = 0.012$ for the temperatures of consideration here, corresponding to the value used in Ref. [117] based on Refs. [123], cf. also [124–126].

If the equilibration is slow compared to the oscillation frequency of the heavy neutrinos, then baryogenesis happens in the oscillatory regime, which includes two steps. First, CP violating oscillations amongst the N_i generate non-zero lepton numbers L_a in the individual flavours, while the total lepton number $L = \sum_a L_a$ remains negligibly small. Later these asymmetries are washed out, primarily by transferring them into helicity asymmetries in the N_i that are invisible to sphalerons. The washout rates $\Gamma_a \simeq (Y^\dagger Y)_{aa} \gamma_{\rm av} T/g_w$ differ for the individual flavours, leading to a net $L \neq 0$ that is partly transferred into B by sphalerons. Here the factor $g_w = 2$ accounts for the fact that $\gamma_{\rm av}$ has been derived in the context of Γ_N, *i.e.* the N_i interact with both components of the SU(2) doublet $\ell_{\rm L}$, while the L_a violating interactions of $\ell_{\rm L}$ only involve the singlet heavy neutrinos. For U^2 in the range close to the naive seesaw relation (19) baryogenesis typically happens in the oscillatory regime.

[8] This implicitly assumes that no N_i are present at the onset of the radiation dominated era.

For large U^2 and small ΔM, as realised in the pseudo-Dirac regime, the equilibration time scale of the more strongly coupled interaction state $N_{\rm s}$ is much faster than the oscillation time scale. This parameter regime can be referred to as the overdamped regime because the BAU is generated within a single overdamped oscillation shortly before sphaleron freezeout.

Quantitatively the SM lepton asymmetries are expressed in terms of the variables $\Delta_a = B/3 - L_a$. The heavy neutrinos can be described in terms of correlation functions in flavour space. Practically we use the quantities $(\delta n_h)_{ij}$, *i.e.* the deviation of the momentum averaged two point correlator between flavour i and j with helicity h from its equilibrium value. The flavour-diagonal, helicity-odd components of this deviation correspond to the *sterile charges* q_{Ni}. At the present level of approximations, this formulation leads to the same results as a description in terms of *density matrices* [127]. We describe the time evolution in terms of the variable $z = T_{\rm ref}/T$, where $T_{\rm ref}$ is an arbitrarily chosen reference temperature which we take to be the temperature $T_{\rm sph}$ of sphaleron freezeout in the following. The time evolution is then given by the set of equations [121]

$$\frac{d}{dz}\delta n_h = -\frac{\mathrm{i}}{2}[H_N^{\rm th} + z^2 H_N^{\rm vac}, \delta n_h] - \frac{1}{2}\{\Gamma_N, \delta n_h\} + \sum_{a,b=e,\mu,\tau} \tilde{\Gamma}_N^a (A_{ab} + C_b/2)\Delta_b \,, \tag{30a}$$

$$\frac{d\Delta_a}{dz} = \frac{\gamma_{\rm av}}{g_w}\frac{a_{\rm R}}{T_{\rm ref}} \sum_i Y_{ia} Y_{ai}^\dagger \left(\sum_b (A_{ab} + C_b/2)\Delta_b - q_{Ni} \right) - 2\frac{\gamma_{\rm av}}{g_w}\frac{a_{\rm R}}{T_{\rm ref}} \sum_{\substack{i,j \\ i\neq j}} Y_{ia}^* Y_{ja} \,. \tag{30b}$$

Here $a_{\rm R} = m_{\rm Pl}\sqrt{45/(4\pi^3 g_*)} = T^2/H$ can be interpreted as the comoving temperature in a radiation dominated universe with Hubble parameter H, $m_{\rm Pl}$ is the Planck mass and g_* is the number of relativistic degrees of freedom in the primordial plasma. The flavour matrix $H_N^{\rm vac}$ can be interpreted as an effective Hamiltonian in vacuum, and $H_N^{\rm th}$ is the hermitian part of the finite temperature correction. The contributions involving the matrix Γ_N and the vector $\tilde{\Gamma}_N$ correspond to collision terms. They are given by

$$H_N^{\rm vac} = \frac{\pi^2}{18\zeta(3)}\frac{a_{\rm R}}{T_{\rm ref}^3}\left({\rm Re}[M^\dagger M] + \mathrm{i}h{\rm Im}[M^\dagger M]\right) \,, \tag{31a}$$

$$H_N^{\rm th} = [\mathfrak{h}_{\rm th} + \mathfrak{h}_{\rm EV}(z)]\frac{a_{\rm R}}{T_{\rm ref}}\left({\rm Re}[Y^* Y^t] - \mathrm{i}h{\rm Im}[Y^* Y^t]\right) \,, \tag{31b}$$

$$\Gamma_N = \gamma_{\rm av}\frac{a_{\rm R}}{T_{\rm ref}}\left({\rm Re}[Y^* Y^t] - \mathrm{i}h{\rm Im}[Y^* Y^t]\right) \,, \tag{31c}$$

$$(\tilde{\Gamma}_N^a)_{ij} = \frac{h}{2}\gamma_{\rm av}\frac{a_{\rm R}}{T_{\rm ref}}\left({\rm Re}[Y_{ia}^* Y_{aj}^t] - \mathrm{i}h{\rm Im}[Y_{ia}^* Y_{aj}^t]\right) \,, \tag{31d}$$

with $\gamma_{\rm av} = 0.012$, $\mathfrak{h}_{\rm EV}(z) = \frac{2\pi^2}{18\zeta(3)}\frac{v^2(z)}{T_{\rm ref}^2}z^2$, $\mathfrak{h}_{\rm th} \approx 0.23$ and $v(z)$ being the z-dependent Higgs field expectation value, for which we use the data presented in Ref. [49]. Finally, the matrix A and vector C are given by

$$A = \frac{1}{711}\begin{pmatrix} -221 & 16 & 16 \\ 16 & -221 & 16 \\ 16 & 16 & -221 \end{pmatrix} \,, \quad C = -\frac{8}{79}\begin{pmatrix} 1 & 1 & 1 \end{pmatrix} \,. \tag{32}$$

At the original scale	M	ΔM^2	$\mathrm{Im}\,\omega$	U_{ai}	$B(z=1)$
Rescaled	ζM	$\eta\Delta M^2$	$\mathrm{Im}\,\omega + \log(\eta/\zeta^3)/6$	$\eta^{1/6}\zeta^{-1}U_{ai}$	$B(\eta^{1/3})\zeta\eta^{-1/3}$

Table 2: *Rescaling of the asymmetry*

These equations can be solved analytically in the two limits

$$\frac{||Y^* Y^t||\gamma_{\rm av} a_{\rm R}^{2/3}}{|M_1^2 - M_2^2|^{1/3}} \begin{cases} \ll 1 & \text{oscillatory} \\ \gg 1 & \text{overdamped} \end{cases}, \tag{33}$$

where $||YY^\dagger||$ refers to the largest eigenvalue of the matrix. The largest values for the U_a^2 consistent with the observed BAU can be found within the overdamped regime. This regime is particularly interesting for two reasons. First, it is naturally realised when $B-L$ is an approximate symmetry, such that at high temperatures $T \gg M_i$ the violation of L is suppressed when comparing to a violation of the individual lepton numbers L_a. Second, as this regime implies large mixings U_a^2, such heavy neutrinos are more likely to be observed in experiments.

A full treatment of the overdamped regime is numerically demanding due to the large separation between the equilibration and oscillation temperatures. However using the semi-analytic approximations developed in Ref. [121], one can remove the degrees of freedom with large equilibration rates by fixing these to their quasi-static values. Then one may numerically solve the remaining set of differential equations, which results in a significantly faster evaluation time. For a subset of parameter choices used here, the semi-analytic solution was compared to the fully numerical result. The fully numerical approach gives a systematically $\sim 50\%$ larger baryon asymmetry, therefore the bounds presented in Figures 4-6, as well as 7-8 may be relaxed accordingly. We further facilitate the numerical analysis using the fact that, for $\epsilon \ll 1$ we can relate solutions for different parameter choices by keeping the full time-dependence of the baryon asymmetry $B(z)$ and using the approximate rescaling property described in Table 2 taken from [121].

We use these approximations to find the maximally allowed U^2 for a given U_a^2/U^2. As choosing $\alpha_{1,2}$ and δ uniquely fixes the ratio U_a^2/U^2, we only need to scan over the remaining free parameters ΔM, ω and the discrete parameter ξ. However we can use the rescaling property to determine the ΔM that gives us the correct BAU by finding the η that solves the equation

$$B(\eta^{1/3})\eta^{-1/3} = B_{\rm observed}\,, \tag{34}$$

and rescale the mass splitting accordingly, which leaves us with optimising U^2 for ω and the discrete parameter ξ only. Note that when rescaling we choose $\zeta = 1$ in this case to keep the absolute mass scale of the RH neutrinos unchanged. By these means we find the upper bounds that are shown in Figures 7-8.

To find the overall bounds for the mixing with individual flavours U_a^2 shown in Figures 4-

6, we first rescale the mass splitting such that the BAU is maximal at the time of freezeout,

$$\frac{\mathrm{d}B(\eta^{1/3})}{\mathrm{d}\eta} = 0\,, \tag{35}$$

and then change the absolute mass scale to get agreement with the observed BAU,

$$\zeta = \frac{\eta^{1/3} B_{\text{observed}}}{B(\eta^{1/3})}\,. \tag{36}$$

However, as we do not fix U_a^2/U^2 in this case, we also need to scan over the parameters $\alpha_{1,2}$, δ, Reω and ξ.

The smallest possible values of U_a^2 lie in a parametric region where neither of the analytic approximations for the oscillatory or overdamped regime apply. Decreasing U_a^2 also decreases the Yukawa couplings Y_{ai} and therefore the baryon asymmetry, which requires for compensation a small mass splitting to produce a resonant enhancement. However, as the oscillations need to happen before the sphaleron freezeout, there is also a lower limit on the mass splitting. This prevents a clear separation between the oscillation, equilibration, and sphaleron freezeout time scales that is required for either of the two regimes to be applicable. Since both the equilibration and oscillation temperatures are comparable in size to the sphaleron freezeout temperature, a fully numerical solution is a viable method for exploring this part of the parameter space, which gives us the lower bounds in Figures 4-6.

3.2 Flavour mixing pattern predictions

In the overdamped regime, the comparably large Yukawa couplings initially lead to the generation of a baryon asymmetry that tends to be much bigger than the observed value but at the same time is subject to a strong washout. Since the damping rates $(\Gamma_N)_{ij}$ of the N_i and the washout rates Γ_a are governed by the same Yukawa couplings, the only way to avoid a complete washout of all lepton asymmetries (and therefore also B) in the overdamped regime is to realise a hierarchy in the magnitude of the washout rates Γ_a for individual SM lepton flavours. Therefore we expect that leptogenesis with large U^2 is only feasible for specific flavour mixing patterns that realise such hierarchy. In the oscillatory regime, on the other had, we do not expect significant constraints on the flavour mixing pattern from leptogenesis, at least not if all of the unknown parameters are allowed to vary freely. In the following we address the question:

If one fixes U^2 to a specific value, for which range of U_a^2/U^2 can the observed BAU be generated?

We use the semi-analytic approach from Ref. [121], as discussed in Subsection 3.1, to impose constraints on the flavour mixing pattern U_a^2/U^2 for N_i with large U^2. We require that the generated BAU lies within a 5σ range of the observed value $\eta_B = (8.06 - 9.11) \times$

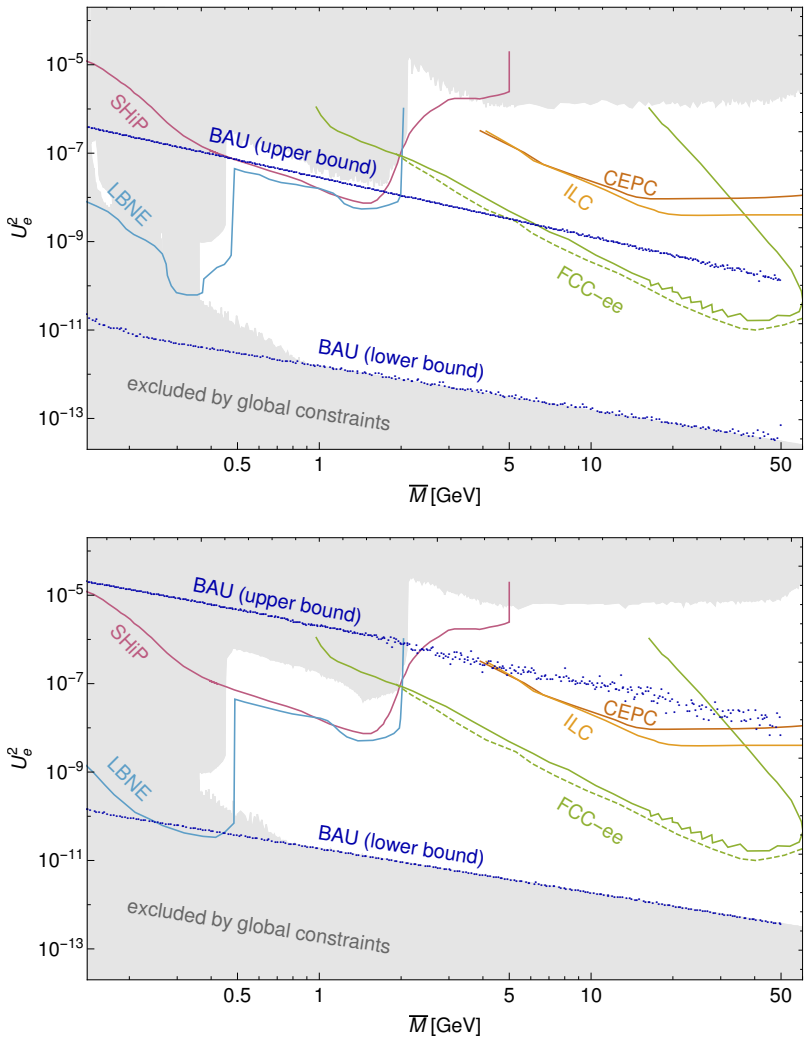

Figure 4: *Limits on U_e^2 as a function of $\bar{M} = (M_1 + M_2)/2$ for normal hierarchy (top panel) and inverted hierarchy (bottom panel). The grey area corresponds to the parameter region that is ruled out by the combined constraints discussed in Subsection 2.3. The dark blue lines are the upper and lower bound of U_e^2 consistent with neutrino oscillation data and the requirement to account for the observed BAU. These are compared to the sensitivity of future experiments: The SHiP lines (purple) show the 90% c.l. upper limits assuming 0.1 background events in 2×10^{20} proton target collisions [51, 128]. The LBNE sensitivity (light blue) is for the assumption of an exposure of 5×10^{21} protons on target for a detector length of 30 m [129]. The solid FCC-ee lines (olive green) correspond to the expected reach of FCC-ee for 10^{12} Z bosons with a displaced vertex at $10 - 100$ cm [130]. The expected sensitivities at 2σ for heavy neutrino searches via displaced vertices are presented for the FCC-ee (olive green, dashed) and the CEPC (brown), both at the Z pole run for a center of mass energy $m_{\rm cms} = m_Z$, and for the ILC (dark orange) for the high-energy run at $m_{\rm cms} = 500$ GeV [131].*

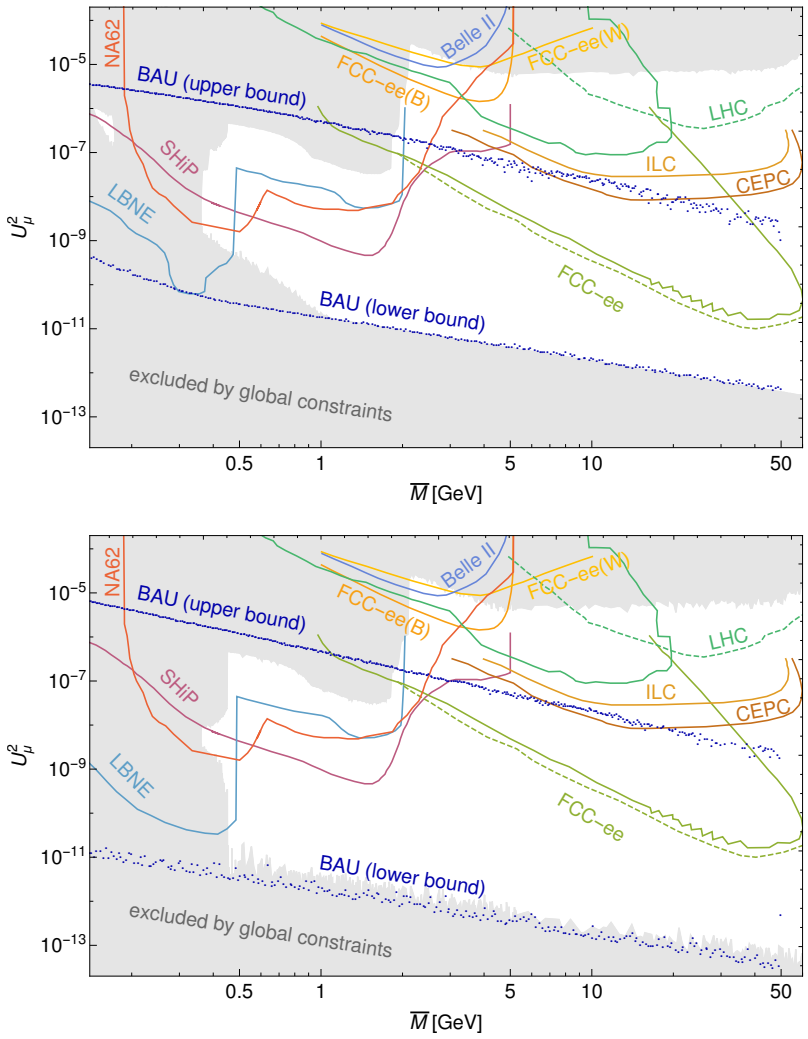

Figure 5: *Limits on U_μ^2 as a function of $\bar{M} = (M_1 + M_2)/2$ for normal hierarchy (top panel) and inverted hierarchy (bottom panel). The grey area corresponds to the parameter region that is ruled out by the combined constraints discussed in Subsection 2.3. The dark blue lines are the upper and lower bound of U_μ^2 consistent with neutrino oscillation data and the requirement to account for the observed BAU. These are compared to the sensitivity of future experiments: The SHiP lines (purple) show the 90% c.l. upper limits assuming 0.1 background events in 2×10^{20} proton target collisions [51, 128]. The LBNE sensitivity (light blue) is for the assumption of an exposure of 5×10^{21} protons on target for a detector length of 30 m [129]. The solid FCC-ee lines (olive green) correspond to the expected reach of FCC-ee for 10^{12} Z bosons with a displaced vertex at $10 - 100$ cm [130]. The expected sensitivities at 2σ for heavy neutrinos searches via displaced vertices are presented for the FCC-ee (olive green, dashed), the CEPC (brown) and for the ILC (dark orange) at the Z pole run for a center of mass energy $m_{\rm cms} = m_Z$ [131]. The NA62 line (dark orange) is the expected limit of the NA62 experiment on U_μ^2 with 2×10^{18} 400 GeV protons on target [132]. Limits on U_μ^2 can be obtained from LNV decays of 5×10^{10} B^+ mesons at Belle II (blue), 10^{13} Z mesons (light orange) and 2×10^8 W bosons (yellow) at the FCC-ee [133]. The turquoise lines are the limits on U_μ^2 from displaced lepton jet (solid) and prompt trilepton (dashed) searches for $\sqrt{s} = 13$ TeV and 300 fb^{-1} at the LHC [134].*

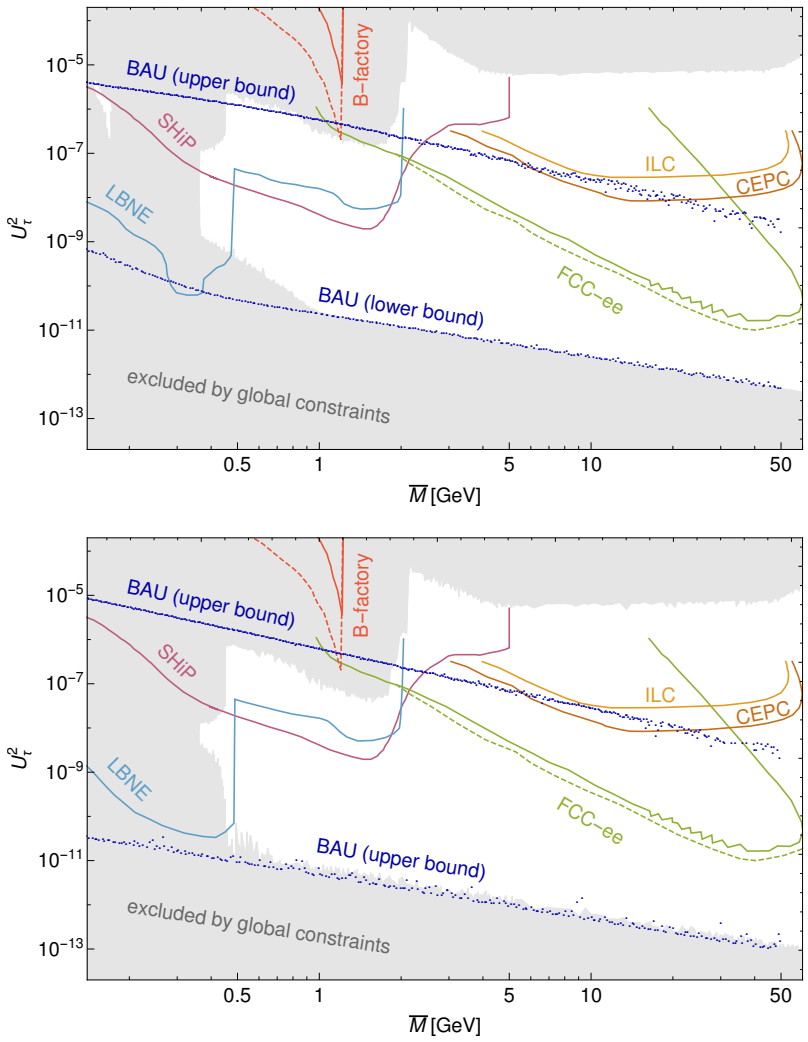

Figure 6: *Limits on U_τ^2 as a function of $\bar{M} = (M_1 + M_2)/2$ for normal hierarchy (top panel) and inverted hierarchy (bottom panel). The grey area corresponds to the parameter region that is ruled out by the combined constraints discussed in Subsection 2.3. The dark blue lines are the upper and lower bound of U_τ^2 consistent with neutrino oscillation data and the requirement to account for the observed BAU. These are compared to the sensitivity of future experiments: The SHiP lines (purple) show the 90% c.l. upper limits assuming 0.1 background events in 2×10^{20} proton target collisions [51, 128]. The LBNE sensitivity (light blue) is for the assumption of an exposure of 5×10^{21} protons on target for a detector length of 30 m [129]. The solid FCC-ee lines (olive green) correspond to the expected reach of FCC-ee for 10^{12} Z bosons with a displaced vertex at $10 - 100$ cm [130]. The expected sensitivities at 2σ for heavy neutrinos searches via displaced vertices are presented for the FCC-ee (olive green, dashed), the CEPC (brown) and for the ILC (dark orange) at the Z pole run for a center of mass energy $m_{\rm cms} = m_Z$ [131]. The conservative (red, solid) and most optimistic (red, dashed) 95% c.l. limits on U_τ^2 at B-factories are shown for a kinematic analysis of 10^6 $\tau^- \to \nu\pi^-\pi^+\pi^-$ decays [135].*

10^{-11} [136]. The results are shown in Figures 7-9. The red region is forbidden because it corresponds to $\sum_a U_a^2/U^2 > 1$. Neutrino oscillation data can be explained within the solid black lines; the dashed lines are iso-U_τ^2/U^2 lines. Increasing the total U^2 makes the washout stronger such that the experimentally measured BAU can just be fulfilled when requiring a strongly flavour asymmetric washout. The coloured regions inside Figures 7-9 illustrate how the allowed region becomes smaller when increasing U^2. Furthermore, it is clearly visible that the maximally achievable U^2 requires a maximally asymmetric washout. For normal hierarchy, *cf.* Figure 7, this happens when the electron couples minimally, $U_e^2/U^2 = 0.0056$, what corresponds to $\alpha_2 = -2\delta + \pi$. In case of inverted hierarchy, *cf.* Figures 8 and 9, maximal mixing is achieved when the electron couples maximally, $U_e^2/U^2 = 0.94$, which corresponds to $\alpha_2 - \alpha_1 = \pi$. These scenarios can are illustrated in Figure 11 and discussed in Appendix A in more detail.

Note that the scenario with equal mixings $U_e^2 = U_\mu^2 = U_\tau^2$ does not allow for leptogenesis because it fails to produce the flavour-asymmetric washout that is required to produce a total $L \neq 0$. For normal hierarchy, this scenario is in any case excluded by neutrino oscillation data, for inverted hierarchy the forbidden region is visible in red in Figure 8.

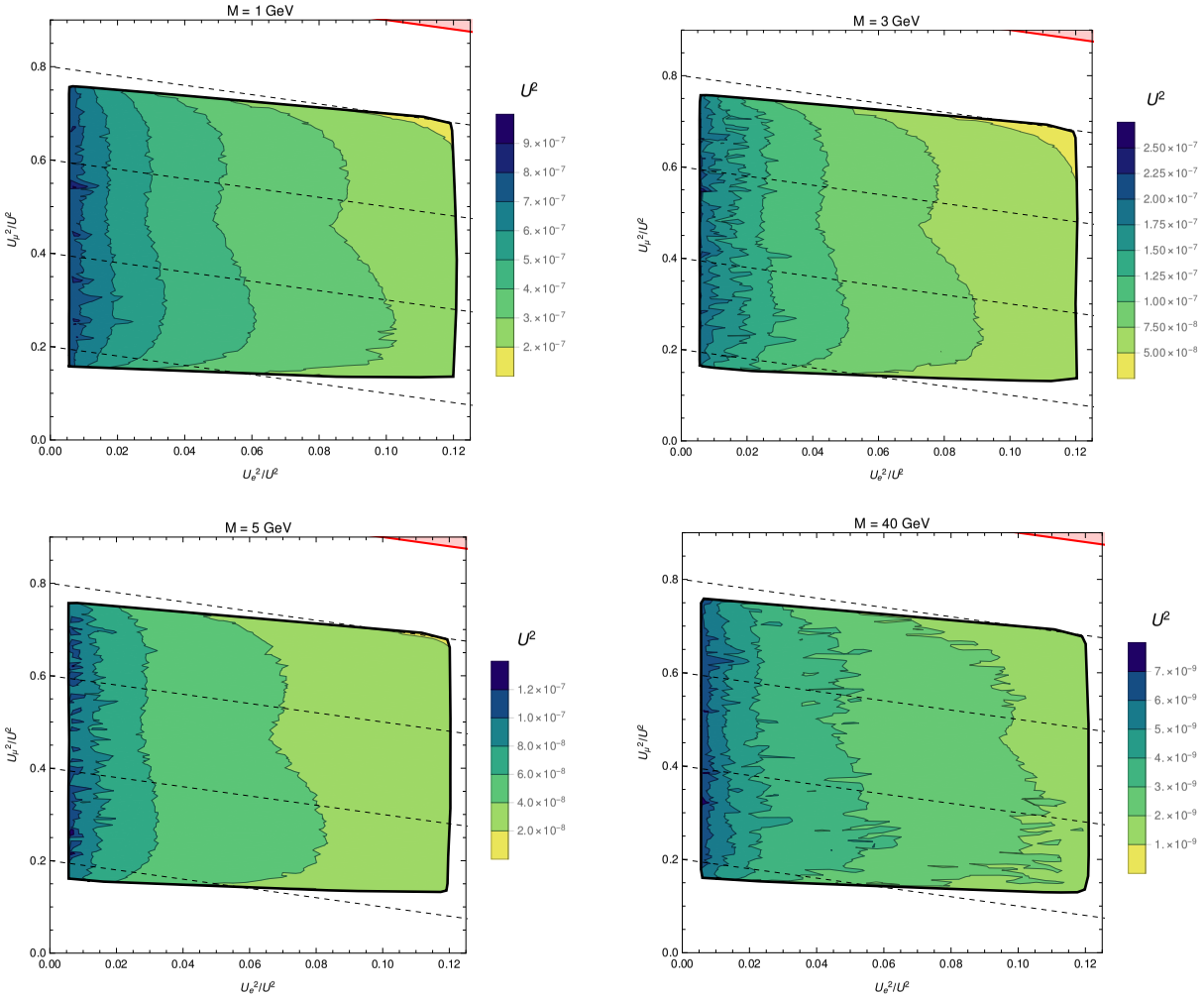

Figure 7: *Maximally allowed U^2 for given U_a^2/U^2 such that the the observed BAU can be generated by leptogenesis. The four plots are for different Majorana masses M_i:* 1 GeV *(top left),* 3 GeV *(top right),* 5 GeV *(bottom left) and* 40 GeV *(bottom right). These plots are shown in the U_e^2/U^2-U_μ^2/U^2 plane for normal hierarchy. The thick black lines display the region consistent with neutrino oscillation data, cf. the top panel of Figure 1. U_τ^2/U^2 is given by the requirement $\sum_a U_a^2/U^2 = 1$ and the iso-U_τ^2/U^2 lines are given by the dashed black lines. The red area indicates the forbidden region $\sum_a U_a^2/U^2 > 1$.*

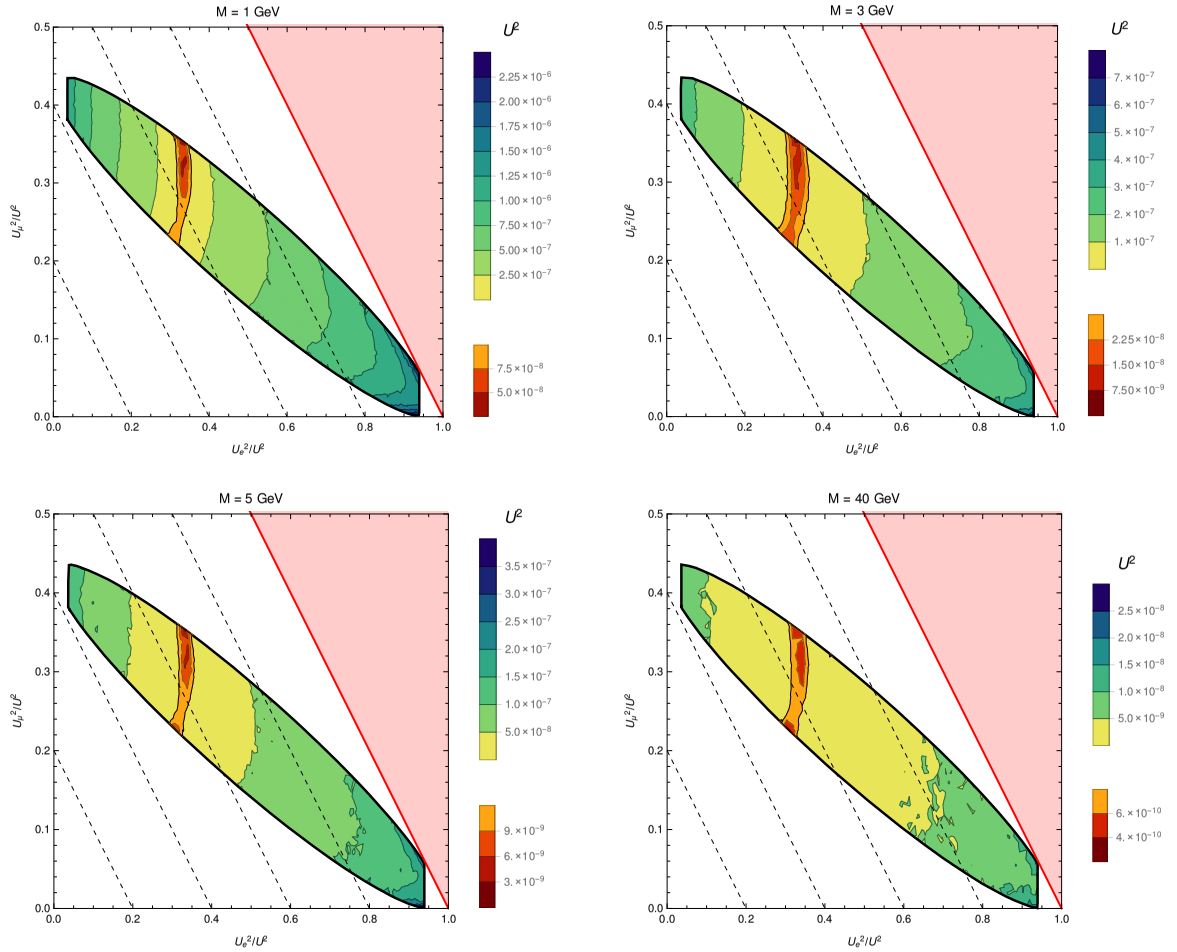

Figure 8: *Same as Figure 7, but for inverted hierarchy. (The thick black lines display the region consistent with neutrino oscillation data, cf. the bottom panel of Figure 1.) The region near the point $U_e^2 = U_\mu^2 = U_\tau^2$ is forbidden because it does not lead to a flavour asymmetric washout, which is required to generate a total $L \neq 0$.*

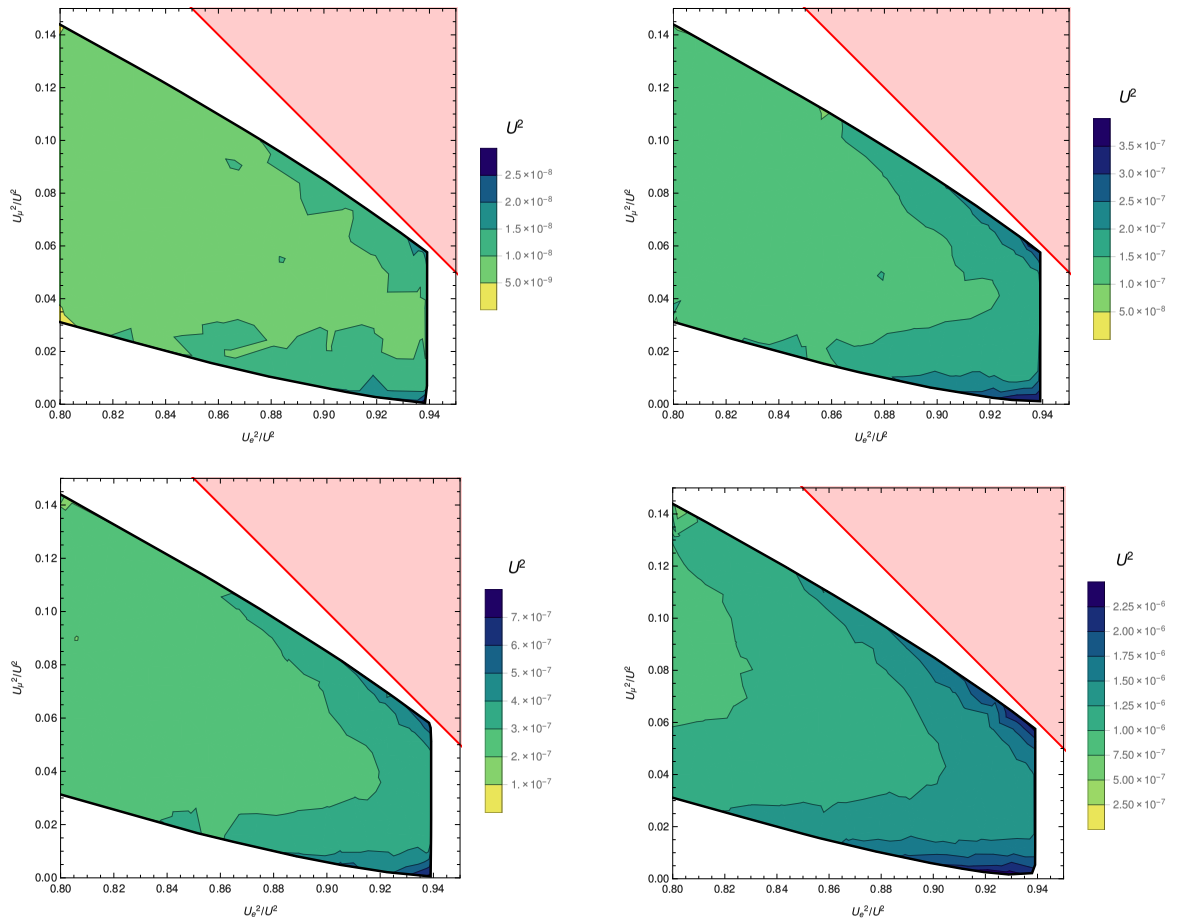

Figure 9: *Magnified view of Figure 8 to show the corner of parameter space that yields maximal mixings U^2 separately for the Majorana masses M_i:* 1 GeV *(top left),* 3 GeV *(top right),* 5 GeV *(bottom left) and* 40 GeV *(bottom right).*

4 Future improvements

In the following we assume that heavy neutral leptons will be found in a direct search experiment. This is the basic requirement for an experimental confirmation of the seesaw mechanism and leptogenesis. Though circumstantial evidence may also come from a combination of indirect signatures, these can always be explained in the framework of effective field theory and are not unique to the seesaw model.

4.1 Direct searches

Heavy neutrinos that are lighter than the W boson can be searched for at both, hadron [104, 105, 134, 137, 138] as well as lepton colliders [130, 131, 139–143]. The reach of the LHC could further be extended with the MATHULSA surface detector [144]. The FCC-ee is expected to probe mixings $U_{ai}^2 < 10^{-9}$ [130, 131] and will have an energy resolution in the sub-MeV range [145]. Consequently, the mass resolution in the search of RH neutrinos will be improved, potentially allowing for a measurement of the individual U_{ai}^2 in the viable parameter space for leptogenesis. It may therefore be capable of a true test of leptogenesis, i.e. a full reconstruction of all fundamental model parameters, which allows to uniquely calculate the value of the BAU and compare it to the observed one.

If the heavy neutrinos are lighter than the B mesons, they can also be searched for at B factories [115, 133, 135, 146, 147] or fixed target experiments [92], including NA62 [132, 148], the SHiP experiment proposed at CERN [51, 52, 140] or a similar setup proposed at the DUNE beam at FNAL [129, 149]. However, even the mass resolution ~ 10 MeV anticipated for SHiP would allow to measure individual U_{ai}^2 only in a small fraction of the viable parameter space.

In the following we assume that at least $\bar{M}$ and all of the U_a^2 can be extracted from the experimental data. This may not be realistic for all experiments (in particular for U_τ^2), but can *e.g.* be done at SHiP. In Section 2 we have shown that for $\epsilon, \mu \ll 1$, a determination of all light neutrino properties allows to uniquely fix the heavy neutrino flavour mixing pattern U_a^2/U^2. In return, a measurement of all mixings U_a^2 already provides a strong test of the hypothesis that the heavy neutral leptons under investigation are part of the seesaw mechanism. In the following we investigate how additional measurements can help to further constrain the parameter space in the limit $\epsilon, \mu \ll 1$. Many experiments are sensitive to more than one parameter. We roughly organise these according to the most important input they can provide, assuming that $\bar{M}$ has been measured and Imω is determined from U^2. We furthermore assume that the Dirac phase δ can be measured in a near future neutrino oscillation experiment, such as DUNE or NOνA. As previously discussed and illustrated in Figure 1, together with measurements of the U_a^2, this provides a strong test of the seesaw relation.

4.2 Heavy neutrino oscillations and CP violation

Measurement of the CP violation in N_i-mediated meson decays – In Refs. [100, 101], it is suggested that the CP violation could be measured in decays mediated by heavy neutrinos of charged pseudoscalar mesons M such as $B^\pm$ and $D^\pm$ into lighter mesons M' and leptons. The CP asymmetry, characterised by the difference between the decay rates of mesons with opposite charge, can be approximated as

$$\mathcal{A}_{CP} \equiv \frac{\sum_i \Gamma(M^- \to \ell_a^- \ell_b^- M'^+) - \Gamma(M^+ \to \ell_a^+ \ell_b^+ M'^-)}{\sum_i \Gamma(M^- \to \ell_a^- \ell_b^- M'^+) + \Gamma(M^+ \to \ell_a^+ \ell_b^+ M'^-)} \approx \frac{y}{y^2+1} \sin\left(\arg\left[\frac{\theta_{a2}}{\theta_{a1}}\frac{\theta_{b2}}{\theta_{b1}}\right]\right), \tag{37}$$

with $y = \Delta M/\bar{\Gamma}_N$ the ratio of the mass splitting and the decay width of the sterile neutrino

$$\bar{\Gamma}_N = \frac{G_F^2 \bar{M}^5}{96\pi^3}\mathcal{N}U^2\,, \tag{38}$$

where $\mathcal{O}(\mathcal{N}) = 10$. In the case of at least two almost mass-degenerate Majorana neutrinos, assuming that their mass splitting ΔM is comparable in size to the decay width $\bar{\Gamma}_N$, the CP violation can become large enough to be measurable, assuming that the initial asymmetry of the produced mesons is under control. As explained in Ref. [100, 101] in more detail, aside from the CP asymmetry $\mathcal{A}_{CP}$, the observation of CP violation also depends on some effective branching ratio, that can be approximated as

$$\mathrm{Br}_{\mathrm{eff}} \sim 10^2 U^4\,. \tag{39}$$

Observing a possible CP violation requires $|\mathcal{A}_{CP}|\mathrm{Br}_{\mathrm{eff}}$ to be larger than the inverse of the number of produced mesons in the experiment. Consequently the size of the CP violating signal is determined by the absolute value of the active sterile mixing angle and thus it is driven by $\mathrm{Im}\omega$. Note however that $\mathrm{Im}\omega$ can already be constrained by a measurement of U_a^2. For $n_s = 2$ sterile neutrinos, two reasons suggest that it appears unlikely that CP violation will be observed experimentally in the parameter region where leptogenesis is feasible.

First, for large mixing angles U^2, there is the relation $\theta_{a2} \simeq \mathrm{i}\theta_{a1}$, and the phase difference in Eq. (37) is given by $\pi/2$, *cf.* Eq. (23). Therefore, in the limit $\epsilon \to 0$, $\mathcal{A}_{CP}$ vanishes, while the first non-vanishing contribution of $\mathcal{A}_{CP}$ is of order ϵ. This suppression has not been considered in Refs. [100, 101] where it is assumed that the sine function in Eq. (37) is approximately one.

Second, there exists no combination of ΔM and U^2 that allows for both leptogenesis and an amount of CP violation observable at SHiP. Setting $y \sim 1$ to maximise CP violation in the mass regime where SHiP could discover heavy neutrinos implies tiny mass splittings $\Delta M/\bar{M} \sim 10^{-15}$ that cannot account for successful leptogenesis. This can be estimated by setting $\bar{\Gamma}_N = \Delta M$ and assuming a SHiP sensitivity of $U^2 \sim 10^{-5}$ at $\bar{M} = 5\,\mathrm{GeV}$. For smaller $\bar{M}$, where the SHiP sensitivity is much better, even smaller values of ΔM are required due to the strong dependence of $\bar{\Gamma} \propto \bar{M}^5$. Note that the resonance condition in

the early universe differs from that in the vacuum as there are thermal corrections to both the heavy neutrino mass splitting as well as to the rate $\bar{\Gamma}_N$. Increasing y to values much larger than unity in order to make leptogenesis possible leads to a suppression $\sim y^{-1}$ of the CP-violating rates in experiments. Keeping $|\mathcal{A}_{CP}|\mathrm{Br}_{\mathrm{eff}}$ in the observable range then requires larger U^2, resulting in a stronger washout, barring successful leptogenesis. We have not found any parameter values for which simultaneously the BAU and an observable $|\mathcal{A}_{CP}|\mathrm{Br}_{\mathrm{eff}}$ at SHiP can be accommodated. Note that we have neglected the Higgs contribution to the heavy neutrino masses, as discussed in Section 2.4, which may not be justified for $\Delta M \lesssim 10^{-11}$.

Measurement of oscillations of the right-handed neutrinos – The mass splitting of heavy neutrinos may be observed as suggested in [102] where two almost degenerate GeV scale sterile neutrinos are considered. Detecting the width of possible semileptonic decays $B \to \mu e \pi$ can give information about the sterile mass splitting. In GeV seesaw models it is the size of the mass splitting that determines the time of the first oscillation of the sterile neutrinos. For $n_s = 2$, highly degenerate sterile neutrinos are favoured for generating large enough mixings U^2 to be detected in future experiments. Consequently, a measurement of the mass splitting may rule out parts of the parameter space. Note that there may be possible corrections if the Higgs term dominates the mass splitting, as discussed in Section 2.4.

Flavour constraints in the oscillatory regime – In the oscillatory regime (or weak-washout regime) of leptogenesis the oscillations of the heavy neutrinos start to happen long before the first heavy neutrino reaches equilibrium as discussed in Section 3. In this regime, the flavoured charge density for a given flavour a are generated at very early times, long before the first heavy neutrino reaches equilibrium and can be approximated as [121]

$$\frac{\Delta_a}{s} \approx -\sum_{\substack{i,j,c \\ i\neq j}} \frac{\mathrm{Im}[Y^\dagger_{ai} Y_{ic} Y^\dagger_{cj} Y_{ja}]}{\mathrm{sign}(M_i^2 - M_j^2)} \left(\frac{m_{\mathrm{Pl}}^2}{|M_i^2 - M_j^2|}\right)^{\frac{2}{3}} \times 3.4 \times 10^{-4} \frac{\gamma_{\mathrm{av}}^2}{g_w}\,, \tag{40}$$

with s the comoving entropy density $s = 2\pi^2 g_\star a_{\mathrm{R}}/45$. This implies that the BAU effectively scales as $B \propto \Delta M^{-2/3}$. For given U^2, a BAU consistent with the observed value can be generated by adjusting the mass difference ΔM. If all U_a^2 are measured, this allows to impose a constraint on the allowed ΔM, as illustrated in Figure 10. Large values of ΔM are only consistent with specific flavour mixing patterns. If ΔM could be measured independently in some way, this can be used as a consistency check for leptogenesis.

4.3 Neutrinoless double beta decay

For heavy neutrino masses and mixings within the reach of fixed target experiments, the rate of $0\nu\beta\beta$ decay can significantly deviate from the standard prediction due to a sizeable

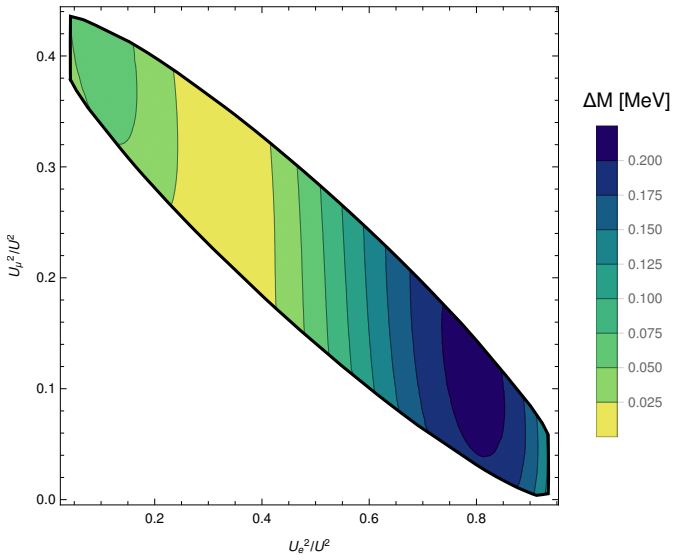

Figure 10: *Maximally allowed mass splitting ΔM for given U_a^2/U^2 such that the observed BAU can be generated by leptogenesis. This is an example plot shown in the U_e^2/U^2-U_μ^2/U^2 plane for inverted hierarchy with a fixed* $\mathrm{Im}\omega = 2 \leftrightarrow U^2 = 5.38 \times 10^{-9}$ *and a mass* $\bar{M} = 0.5\,\mathrm{GeV}$. *The thick black lines enclose the region within which neutrino oscillation data can be explained, cf. the bottom panel of Figure 1. U_τ^2/U^2 is given by the requirement* $\sum_a U_a^2/U^2 = 1$.

contribution from heavy neutrino exchange [150]. The rate of $0\nu\beta\beta$ decay can be expressed in terms of the *effective Majorana mass*

$$\begin{aligned} m_{\beta\beta} &= \left| \sum_i (U_\nu)_{ei}^2 m_i + \sum_i \Theta_{ei}^2 M_i f_A(M_i) \right| \\ &= \left| [1 - f_A(\bar{M})] m_{\beta\beta}^\nu + \sum_i M_i \Theta_{ei}^2 [f_A(M_i) - f_A(\bar{M})] \right| . \end{aligned} \tag{41}$$

The first term in the first line is the contribution from the exchange of light neutrinos,

$$m_{\beta\beta}^\nu = \sum_i (U_\nu)_{ei}^2 m_i \,, \tag{42}$$

whereas the second term is due to the exchange of heavy neutrinos. Since the typical momentum exchange of $0\nu\beta\beta$ is $\Lambda \sim 100\,\mathrm{MeV}$, masses M_i larger than this scale make the exchanged heavy neutrinos virtual and lead to a contact interaction. The resulting suppression is parametrised by the function f_A, for which we here use the *Argonne model* as discussed in Ref. [151],

$$f_A(M) \simeq \left. \frac{\Lambda^2}{\Lambda^2 + M^2} \right|_{\Lambda^2 = (0.159\,\mathrm{GeV})^2} . \tag{43}$$

To first order in ΔM, one can express Eq. (41) as

$$m_{\beta\beta} \simeq \left| [1 - f_A(\bar{M})] m^{\nu}_{\beta\beta} + 2 f_A^2(\bar{M}) \frac{\bar{M}^2}{\Lambda^2} \Delta M (\Theta^2_{e1} - \Theta^2_{e2}) \right| . \tag{44}$$

For $m_{\rm lightest} = 0$ and $m^2_{\rm atm} \gg m^2_{\rm sol}$, as well as in the limit $\epsilon \ll 1$, one finds $\Theta_{e2} \approx \theta_{e2} = \mathrm{i}\theta_{e2} \approx \mathrm{i}\Theta_{ea}$, such that $\Theta^2_{e1} - \Theta^2_{e2} \approx 2\theta^2_{e1}$. Consequently, the expressions for the two hierarchies can be recast in terms of the Casas-Ibarra parameters

$$m^{\rm NO}_{\beta\beta} \simeq \left| [1 - f_A(\bar{M})] m^{\nu}_{\beta\beta} + f_A^2(\bar{M}) \frac{\bar{M}^2}{\Lambda^2} \frac{\Delta M}{\bar{M}} |m_{\rm atm}| e^{2\mathrm{Im}\omega} e^{-2\mathrm{i}(\mathrm{Re}\omega + \delta)} \right| , \tag{45a}$$

$$\begin{aligned} m^{\rm IO}_{\beta\beta} \simeq \Bigg| & [1 - f_A(\bar{M})] m^{\nu}_{\beta\beta} + f_A^2(\bar{M}) \frac{\bar{M}^2}{\Lambda^2} \frac{\Delta M}{\bar{M}} |m_{\rm atm}| \cos^2\theta_{13} \\ & \times e^{2\mathrm{Im}\omega} e^{-2\mathrm{i}\mathrm{Re}\omega} (\xi e^{\mathrm{i}\alpha_2/2} \sin\theta_{12} + \mathrm{i} e^{\mathrm{i}\alpha_1/2} \cos\theta_{12})^2 \Bigg| . \end{aligned} \tag{45b}$$

In order to make predictions about the heavy neutrino parameters, the terms involving f_A in Eqs. (45) for each hierarchy need to be comparable to the experimental sensitivity, which implies that $\bar{M}$ is not too much larger than Λ. For $\bar{M} \sim 1$ GeV and $\Delta M > 10^{-4}$ GeV, an enhanced rate of $0\nu\beta\beta$ can be achieved while reproducing the correct value for the BAU [46, 49, 152]. This does not only allow to constrain the phases in U_ν, $\mathrm{Im}\omega$ and ΔM but also the parameter $\mathrm{Re}\omega$, which is otherwise difficult to access. For small values of ΔM, $m_{\beta\beta}$ is given by $m_{\beta\beta} \simeq \left|[1 - f_A(\bar{M})] m^{\nu}_{\beta\beta}\right|$ [44, 153]. In this case it still provides a useful probe of the Majorana phase and $\bar{M}$, even if U^2 is too small for a direct measurement of $\bar{M}$. For inverted hierarchy $\mathrm{Re}\omega$ can in principle be extracted from $0\nu\beta\beta$ decay as all other parameters can be measured. However, the second term in Eq. (45b) is suppressed for large $\bar{M}$, such that the sensitivity to $\mathrm{Re}\omega$ is swamped in the error bars of the experiment. It has been previously argued in Ref. [46, 49, 152] that a meaningful constraint on $\mathrm{Re}\omega$ can be inferred from $0\nu\beta\beta$ decay if $\bar{M}$ is smaller than a few GeV.

4.4 The $\mu \to e\gamma$ rare lepton decay

The decay rate $\Gamma_{\ell_a \to \ell_b + \gamma}$ of radiative rare lepton decays $\ell_a \to \ell_b + \gamma$ is given by [154, 155]

$$\Gamma_{\ell_a \to \ell_b + \gamma} = \frac{\alpha_{\rm em} m_a^5 G_\mu^2}{2048\pi^4} |R_{ab}|^2 , \tag{46}$$

with $G_\mu \simeq G_F (V_\nu V_\nu^\dagger)_{ee} (V_\nu V_\nu^\dagger)_{\mu\mu}$ a modified Fermi constant G_F that is measured via the lifetime of the μ and affected by the existence of sterile neutrinos. Here

$$R_{ab} = \sum_j (V_\nu^*)_{bj} (V_\nu)_{aj} G\left(\frac{m_j^2}{M_W^2}\right) + \sum_i \Theta^*_{bi} \Theta_{ai} G\left(\frac{M_i^2}{M_W^2}\right) , \tag{47}$$

where the second term is due to an exchange of heavy neutrinos in the loop. The function taking account of the loop contributions is

$$G(x) = \frac{10 - 43x + 78x^2 - 49x^3 + 4x^4 + 18x^3 \log(x)}{3(x-1)^4}. \tag{48}$$

The experimentally most constrained process is $\mu \to e\gamma$ with a branching ratio of [86]

$$B(\mu \to e\gamma) = \frac{\Gamma(\mu \to e\gamma)}{\Gamma(\mu \to e\nu_\mu \bar{\nu}_e)} < 5.7 \times 10^{-13}\,. \tag{49}$$

With Eq. (46) one can express the branching ratio as follows

$$B(\mu \to e\gamma) = \frac{\alpha_{\rm ew}}{32\pi} |R_{e\mu}|^2\,. \tag{50}$$

If all (heavy and light) neutrinos had the same mass, then the function G would be a constant, and $R_{e\mu}$ would vanish due to the unitarity of the full 5×5 neutrino mixing matrix. This *GIM suppression* is the reason why the rate of the decay $\mu \to e\gamma$ in the SM without heavy neutrinos is extremely small, as the deviation of G from the constant value $G(0) = 10/3$ is tiny ($\mathcal{O}[m_i^2/M_W^2] < 10^{-23}$) such that we may approximate

$$|R_{e\mu}| \approx \sum_i \left|\theta_{ei}\theta_{i\mu}^\dagger\right| \left[G\left(\frac{M_i^2}{M_W^2}\right) - \frac{10}{3}\right]\,. \tag{51}$$

One can express Eq. (51) in terms of the Casas-Ibarra parameters

$$|R_{e\mu}| \approx \frac{1}{2\bar{M}} \left[G\left(\frac{M_i^2}{M_W^2}\right) - \frac{10}{3}\right] m_{\rm atm} e^{2{\rm Im}\omega} \sin\theta_{13} \cos\theta_{13} \sin\theta_{23}\,, \tag{52}$$

which is true for both hierarchies and in the limits $m_{\rm sol}^2/m_{\rm atm}^2 \ll 1$, ${\rm Im}\omega \gg 1$ and $\Delta M/\bar{M} \ll 1$ for degenerate masses $M_1 \approx M_2 \approx \bar{M}$. While the branching ratio is thus $\propto 1/\epsilon$, it is nonetheless bounded from above due to the direct upper bounds on the U_a^2. For $\bar{M} \ll M_W$ future searches for lepton flavour violating decays are therefore unlikely to lead to additional constraints on the model parameters. In the regime $\bar{M} \sim M_W$ a discovery of $\mu \to e\gamma$ is possible because G in Eq. (52) deviates substantially from 10/3 and the direct bounds on the U_a^2 are weaker. The rate for $\mu \to e\gamma$ would then be sensitive to the same parameters $\bar{M}$, ${\rm Im}\omega$ as the observables U_a^2, *cf.* Eq. (52).

4.5 Measurement of lepton universality violation

A violation of lepton universality can be described by comparing decays of a particle X (which can be a meson M or a τ-lepton) into leptons of different flavours $a \neq b$ [41, 156]:

$$R_{ab}^M = \frac{\Gamma(M^+ \to \ell_a^+ \nu_a)}{\Gamma(M^+ \to \ell_b^+ \nu_b)}\,, \qquad\qquad R_{ab}^\tau = \frac{\Gamma(\tau^+ \to \ell_a^+ \nu_a \bar{\nu}_\tau)}{\Gamma(\tau^+ \to \ell_b^+ \nu_b \bar{\nu}_\tau)}\,. \tag{53}$$

A sensitive observable is the deviation from the SM prediction, that is given by [41]

$$\Delta r_{ab}^X = \frac{R_{ab}^X}{R_{ab\,\mathrm{SM}}^X} - 1\,. \tag{54}$$

A decomposition of Eq. (53) into mass eigenstates yields in case of the mesons

$$R_{ab}^M = \frac{\sum_i \Gamma(M^+ \to \ell_a^+ \nu_i) + \sum_i \Gamma(M^+ \to \ell_a^+ N_i)}{\sum_i \Gamma(M^+ \to \ell_b^+ \nu_i) + \sum_i \Gamma(M^+ \to \ell_b^+ N_i)}\,, \tag{55}$$

with an analogous equation for the τ. We use the deviation

$$\Delta r_{ab}^X = \frac{\sum_c |(V_\nu)_{ac}|^2 + \sum_i U_{ai}^2 G_{ai}}{\sum_c |(V_\nu)_{bc}|^2 + \sum_i U_{ai}^2 G_{bi}} - 1 = \frac{1 + \sum_i U_{ai}^2 [G_{ai} - 1]}{1 + \sum_i U_{bi}^2 [G_{bi} - 1]} - 1\,, \tag{56}$$

where

$$G_{ai} = \vartheta(m_X - m_{\ell_a} - M_i) \frac{r_a + r_i - (r_a - r_i)^2}{r_a (1 - r_a)^2} \sqrt{1 - 2(r_a + r_i) + (r_a - r_i)^2}\,, \tag{57}$$

with $r_a = m_{\ell_a}^2 / m_X^2$ and $r_i = M_i^2 / m_X^2$. Note that, even if the decaying particle X is lighter than the heavy neutrinos, such that the latter do not appear as final states and $G_{ai} = 0$, the decay can be affected indirectly due to a unitarity violation of V_ν and yields

$$\Delta r_{ab}^X = \frac{\sum_c |(V_\nu)_{ac}|^2}{\sum_c |(V_\nu)_{bc}|^2} - 1 = \frac{1 - U_a^2}{1 - U_b^2} - 1 \simeq U_b^2 - U_a^2\,. \tag{58}$$

For kaon decay the result from NA62 [79] compared to the SM prediction [157] is

$$R_{e\mu}^K = (2.488 \pm 0.010) \times 10^{-5}\,, \tag{59a}$$

$$R_{e\mu\,\mathrm{SM}}^K = (2.477 \pm 0.001) \times 10^{-5}\,, \tag{59b}$$

while from pion [80] and tauon decay [81, 158] we obtain

$$R_{e\mu}^\pi = (1.230 \pm 0.004) \times 10^{-4}\,, \tag{60a}$$

$$R_{e\mu\,\mathrm{SM}}^\pi = (1.2354 \pm 0.0002) \times 10^{-4}\,, \tag{60b}$$

and

$$R_{e\mu}^\tau = 0.9764 \pm 0.0030\,, \tag{61a}$$

$$R_{e\mu\,\mathrm{SM}}^\tau = 0.973\,, \tag{61b}$$

with deviations $|\Delta r_{e\mu}^X| \simeq 5 \times 10^{-3}$ for these three decay channels. In the following we make an estimate of the theory prediction for $|\Delta r_{e\mu}^X|$. For simplicity we neglect G from Eq. (57)

and note that this can lead to an $\mathcal{O}(1)$ error but does not affect our estimate given the necessary accuracy. $|\Delta r^X_{e\mu}|$ can then be expressed in terms of the Casas-Ibarra parameters

$$|\Delta r^X_{e\mu}| \simeq |U_\mu^2 - U_e^2| \simeq \begin{cases} e^{2\mathrm{Im}\omega}\frac{m_{\mathrm{atm}}}{2\bar{M}}\cos^2\theta_{13}\sin^2\theta_{23} & \text{for NO} \\ e^{2\mathrm{Im}\omega}\frac{m_{\mathrm{atm}}}{4\bar{M}}\left|1+3\xi\sin(\frac{\alpha_2-\alpha_1}{2})\sin 2\theta_{12}\right| & \text{for IO} \end{cases} . \tag{62}$$

Here we have used Eqs. (26) and (27) as well as the relative smallness of θ_{13} compared to θ_{23}, $|\mathrm{Im}\omega| \gg 1$ and further limited ourselves to the $n_s = 2$ mass degenerate case, where we have additionally neglected the mass splitting ΔM. Note that the SM expectation $\Delta r^X_{e\mu\,\mathrm{SM}} = 0$ is in slight tension with the experimentally measured values, however, it is within the 2σ range. We can further approximate the theory prediction $|\Delta r^X_{e\mu}| \simeq |U_\mu^2 - U_e^2| < U^2$, that has to be smaller than 10^{-5} in order to be consistent with leptogenesis constraints [121]. This also is in tension but again remains in the 2σ range of the measured value. Future experiments with increased sensitivity may yield constraints on $\mathrm{Im}\omega$, the Majorana mass $\bar{M}$ and the phase difference $\alpha_2 - \alpha_1$.

5 Conclusions

The extension of the SM by two RH neutrinos with masses below the electroweak scale can simultaneously explain the observed neutrino masses via the seesaw mechanism and the BAU via low scale leptogenesis. In addition to the light neutrino masses m_i and mixing matrix U_ν, this model adds only four new parameters to the SM: The masses M_1 and M_2 of the heavy neutrinos and a complex angle ω, which determines the misalignment between the heavy neutrino mass and interaction basis as well as the overall strength $U^2 = \sum_{a=e,\mu,\tau} U_a^2$ of the mixing of the heavy neutrinos with the SM neutrinos. Here $U_a^2 = \sum_i U_{ai}^2$ is the sum of the mixings of both heavy neutrino states N_i with the SM flavour a. Leptogenesis with two RH neutrinos requires a mass degeneracy between these. Because of this, it is convenient to use the average mass $\bar{M}$ and mass splitting ΔM of the two heavy neutrinos instead of their individual masses M_1 and M_2.

Eqs. 17) and (18) show that, for given neutrino mass spectrum, the overall coupling strength U^2 of the heavy neutrinos is determined by the complex parameter ω alone. Assuming that the full neutrino mass spectrum is known and the Dirac phase δ is measured, there are only three free parameters: the real and imaginary parts of ω and a combination of Majorana phases in the light neutrino mixing matrix. Measurements of all individual U_{ai}^2 would allow to overconstrain the parameter space of the seesaw model. At the same time, this also allows to uniquely calculate the BAU generated by the heavy neutrinos from observed quantities. If heavy neutral leptons are found in future experiments, this allows to independently confirm the hypotheses that these are indeed the (sole) origin of neutrino masses and the baryonic matter in the universe. This would *e.g.* be possible at FCC-ee, which aims at a sub-MeV mass resolution and may observe enough events to reconstruct the real and imaginary parts of ω from Eqs. (17) and (18). For $\Delta M > 10$ MeV it is also possible at SHiP.

However, in most of the parameter region where the observed BAU can be reproduced by two heavy neutrinos, their masses are required to be too degenerate to be resolved experimentally by SHiP or any existing experiment. This does not only make a direct determination of ΔM impossible, but also implies that the mixings U_{a1}^2 and U_{a2}^2 of the two heavy neutrinos with the different SM generations cannot be measured individually. Instead, experiments can only constrain their sum U_a^2. Moreover, values of U^2 that lie within reach of realistic experiments that can be realised without a high energy lepton collider require comparably large values of $\mathrm{Im}\omega$. In the parameter region with $\Delta M/\bar{M} \ll 1$ and $\mathrm{Im}\omega > 1$, the sensitivity of U^2 to $\mathrm{Re}\omega$ is practically lost. Hence, the two parameters ΔM and $\mathrm{Re}\omega$, which are crucial for leptogenesis, cannot be determined by neutrino oscillation data and direct searches for the N_i alone. Hence, leptogenesis in this scenario is not fully testable by data from SHiP and DUNE (in the sense that the BAU can be calculated from measured quantities).

However, our analysis shows that even without FCC-ee, the parameter space of the model can be severely constrained, and testable predictions can be made based on the requirement to explain the observed BAU.

- In the limit $\Delta M/\bar{M} \ll 1$ and $\mathrm{Im}\omega \gg 1$, the flavour mixing pattern U_a^2/U^2 of the heavy neutrinos is determined by light neutrino parameters alone. With the exception of one Majorana phase, all of these may be measured in foreseeable time. The precise relations are given in Appendix A. This point has recently also been made in Ref. [46]. Even in the limit $\Delta M/\bar{M} \ll 1$ and $\mathrm{Im}\omega > 1$, the seesaw relation can be overconstrained by independent determinations of all U_a^2 and the Dirac phase δ, using the relations derived in Section 2. While δ is expected to be measured by the next generation of neutrinos oscillation experiments, all three U_a^2 could be determined at SHiP.

- By combining the negative results of various direct and indirect search experiments with constraints from BBN, one can impose considerably stronger bounds on the U_a^2 than by simply superimposing them. We present the results of the first global analysis of this kind in Figures 2 and 3.

  - The combined constraints rule out most of the parameter region below $\bar{M} \simeq 350$ MeV. Moreover, they impose a much stronger lower bound on U_μ^2 and U_τ^2 than BBN and the seesaw relation alone for $\bar{M} < m_K$. However, before completely disregarding the mass region $\bar{M} < 350$ MeV, a careful re-analysis of the lower bounds on U_a^2 from BBN should be performed in the regime $\bar{M} > m_\pi$.[9] In this work, we used the simple estimate that the heavy neutrino lifetime should be shorter than 0.1s, which may be too simplified. Moreover, there exist different interpretations of the results of the PS191 experiment in the literature [45, 65, 69], and the combined constraints strongly depend on these differences. In our analysis we have chosen to use the results of Ref. [45]. Finally, we have fixed the

[9] For masses $\bar{M} < m_\pi$ a revised calculation has recently been presented in Ref. [94], where the authors also perform a comparison to earlier results in the literature.

known neutrino masses and mixing angles to their best fit values in Figures 2 and 3. The error bars on these quantities should slightly relax the exclusion bounds presented there.

  - In the regime $m_K < \bar{M} < m_D$ the combined constraints impose a much stronger upper bound on U_τ^2 than those from direct searches alone. For normal hierarchy, they impose a stronger upper bound on U_e^2.
  - Any improvement in the measurement of light neutrino properties will tighten the combined constraints. In particular, a measurement of the Dirac phase δ and the light neutrino mass hierarchy would be highly desirable.
  - It should be pointed out that the combined constraints are specific to the minimal scenario with two mass degenerate heavy neutrinos or models that can effectively be described in this way (*e.g.* the νMSM). They are considerably weaker if more heavy neutrinos exist in the mass range we consider or the masses are not degenerate [13].

- Even in the case $\Delta M/\bar{M} \ll 1$ and $\mathrm{Im}\omega \gg 1$, in which the values of ΔM and $\mathrm{Re}\omega$ cannot be extracted from measurements of the U_{ai}^2, a measurement of the individual U_a^2 still provides a powerful test of the minimal low scale leptogenesis scenario. As shown in Section 3, the requirement to explain the observed BAU allows to make predictions for the flavour mixing pattern U_a^2/U^2 for given $\bar{M}$ and U^2. Finding heavy neutral leptons with flavour mixing patterns within these regions will provide circumstantial evidence for leptogenesis.

- As shown in Section 4, full testability of the leptogenesis mechanism can be achieved in the parameter region with $\Delta M/\bar{M} \ll 1$ and $\mathrm{Im}\omega > 1$ if other experimental data is added. For $\bar{M}$ below $1 - 2$ GeV, a measurement of neutrinoless double β decay can provide information about $\mathrm{Re}\omega$. Moreover, various processes that are sensitive to the oscillations of heavy neutrinos in the laboratory and the degree of lepton number violation they mediate can be used to extract information about ΔM. However, as pointed out in Sec. 2.4, a quantitative analysis requires careful inclusion of $\mathcal{O}[U^2]$ corrections to the heavy neutrino mass spectrum at tree level as well as loop corrections.

- In Figures 4, 5 and 6 we present estimates for the range of allowed values for the mixings U_a^2 of heavy neutrinos with individual SM flavours that are consistent with successful leptogenesis and compare these to the expected sensitivity of planned experiments. These results may be used to estimate the discovery potential of experiments that are only sensitive to one or two SM flavours, or which have very different sensitivities to the individual flavours. These results may be compared to those found in Ref. [46], which appear much more pessimistic. The reason for the apparent discrepancy may lie in the fact that the authors of that study performed a Bayesian analysis to estimate the likelihood that heavy neutrinos with given parameters are

responsible for the BAU. While such analysis in principle allows to different information about the parameter space, this additional information in the present case clearly depends on the choice of the choice of parametrisation and priors. In contrast, our analysis aims at identifying the largest and smallest U_a^2 that are consistent with neutrino oscillation data and successful leptogenesis, without imposing any theoretical prejudice about the model parameters. In this sense, the two analyses should be viewed as complementary.

In conclusion, the low scale seesaw and leptogenesis provide a simple explanation for at least two of the most studied questions in fundamental physics, the origin of neutrino masses and the origin of the baryonic matter in the universe. A significant fraction of the parameter space can be tested in existing or proposed experiments. The global constrains and estimates of the cosmologically relevant parameter space presented here are state of the art, but still suffer from order one uncertainties. In the wake of upcoming experiments, further theoretical work will be necessary to reduce these to a level that would be required for a comparison with experimental data if any heavy neutral leptons are discovered.

Acknowledgements

We would like to thank Elena Graverini, Walter Bonivento, Gaia Lanfranchi, Oliver Fischer and Jilberto Antonio Zamora Saa for helpful discussions about experimental aspects. This research was supported by the DFG cluster of excellence 'Origin and Structure of the Universe' (www.universe-cluster.de).

A Heavy neutrino mixing angles

In the following we write down analytic expressions for the flavour mixings U_a^2 for both the normal and the inverted hierarchy. We limit ourselves to the parametric region where leptogenesis makes flavour predictions for the active-sterile mixing, namely the overdamped regime. In this case, in order to fulfil leptogenesis constraints, it is required to have large $\mathrm{Im}\omega$ and high degeneracies, *i.e.* we neglect μ, such that $M_1 \simeq M_2 \simeq \bar{M}$, and only keep terms of order $1/\epsilon$, *cf.* Eq. (22). The masses of the three SM neutrinos are denoted by m_i, s_{ij} and c_{ij} are shorthand notations for $\sin\theta_{ij}$ and $\cos\theta_{ij}$, respectively, with the neutrino mixing angles θ_{ij} for $i, j = 1, 2, 3$. Experimental values are given in Table 1. As we are dealing with $n_s = 2$ sterile neutrinos, the lightest neutrino mass has to be zero. The following expressions are given in terms of the Casas-Ibarra parameters, *cf.* Subsection 2.1.

Normal hierarchy:

$$U_e^2 \approx \frac{e^{2\mathrm{Im}\omega}}{2\bar{M}} \left[a_1 - a_2 \sin\left(\frac{\alpha_2}{2} + \delta\right) \right] , \tag{63a}$$

$$U_\mu^2 \approx \frac{e^{2\mathrm{Im}\omega}}{2\bar{M}} \left[a_3 - a_4 \cos(\delta) - a_5 \sin\left(\frac{\alpha_2}{2}\right) + a_6 \sin\left(\frac{\alpha_2}{2} + \delta\right) \right] , \tag{63b}$$

$$U_\tau^2 \approx \frac{e^{2\mathrm{Im}\omega}}{2\bar{M}} \left[a_7 + a_8 \cos(\delta) + a_9 \sin\left(\frac{\alpha_2}{2}\right) + a_{10} \sin\left(\frac{\alpha_2}{2} + \delta\right) \right] , \tag{63c}$$

with a_1 to a_9 positive values given by active neutrino masses and their mixing angles:

$$\begin{aligned}
a_1 &= m_2 c_{13}^2 s_{12}^2 + m_3 s_{13}^2 \,, \\
a_2 &= 2\sqrt{m_2 m_3} c_{13} s_{12} s_{13} \xi \,, \\
a_3 &= m_2 (c_{12}^2 c_{23}^2 + s_{12}^2 s_{13}^2 s_{23}^2) + m_3 c_{13}^2 s_{23}^2 \,, \\
a_4 &= 2 m_2 c_{12} c_{23} s_{12} s_{13} s_{23} \,, \\
a_5 &= 2\sqrt{m_2 m_3} c_{12} c_{13} c_{23} s_{23} \xi \,, \\
a_6 &= 2\sqrt{m_2 m_3} c_{13} s_{12} s_{13} s_{23}^2 \xi \,, \\
a_7 &= m_2 (c_{23}^2 s_{12}^2 s_{13}^2 + c_{12}^2 s_{23}^2) + m_3 c_{13}^2 c_{23}^2 \,, \\
a_8 &= a_4 \,, \\
a_9 &= a_5 \,, \\
a_{10} &= 2\sqrt{m_2 m_3} c_{13} c_{23}^2 s_{12} s_{13} \xi \,.
\end{aligned} \tag{64}$$

Due to the fact that for normal hierarchy we have $m_1 = 0$, Eq. (63) and thus the mixings do not depend on α_1, which is why we can use $\alpha_1 = 0$.
On the one hand, the minimal electron (relative) mixing angle $U_e^2/U^2 = 0.00557$, which turns out to maximise U^2 under the condition of fulfilling leptogenesis constraints[10], is obtained by the choice $\alpha_2 = -2\delta + \pi$. The maximal μ and τ (relative) mixing U_μ^2/U^2 and U_τ^2/U^2 are given by $\delta = \pi$ and $\delta = 0$ with this particular value of α_2, respectively. On the other hand it is worth mentioning that the maximal electron (relative) mixing occurs for $\alpha_2 = -2\delta + 3\pi$, while the maximal μ and τ (relative) mixing U_μ^2/U^2 and U_τ^2/U^2 for $\delta = 0$ and $\delta = \pi$, respectively, with this value of α_2. Note that maximal muon mixing corresponds to minimal tauon mixing and vice versa as the plot for the relative mixings for normal hierarchy in the upper panel of Figure 11 demonstrates.

[10]In fact, the maximal possible total mixing U^2 in NO is obtained for the minimal electron relative mixing U_e^2/U^2. However, this is not necessarily true for a given mass splitting ΔM, as it is the case for $\Delta M \lesssim 10^{-10}$ with $M = 1\,\mathrm{GeV}$.

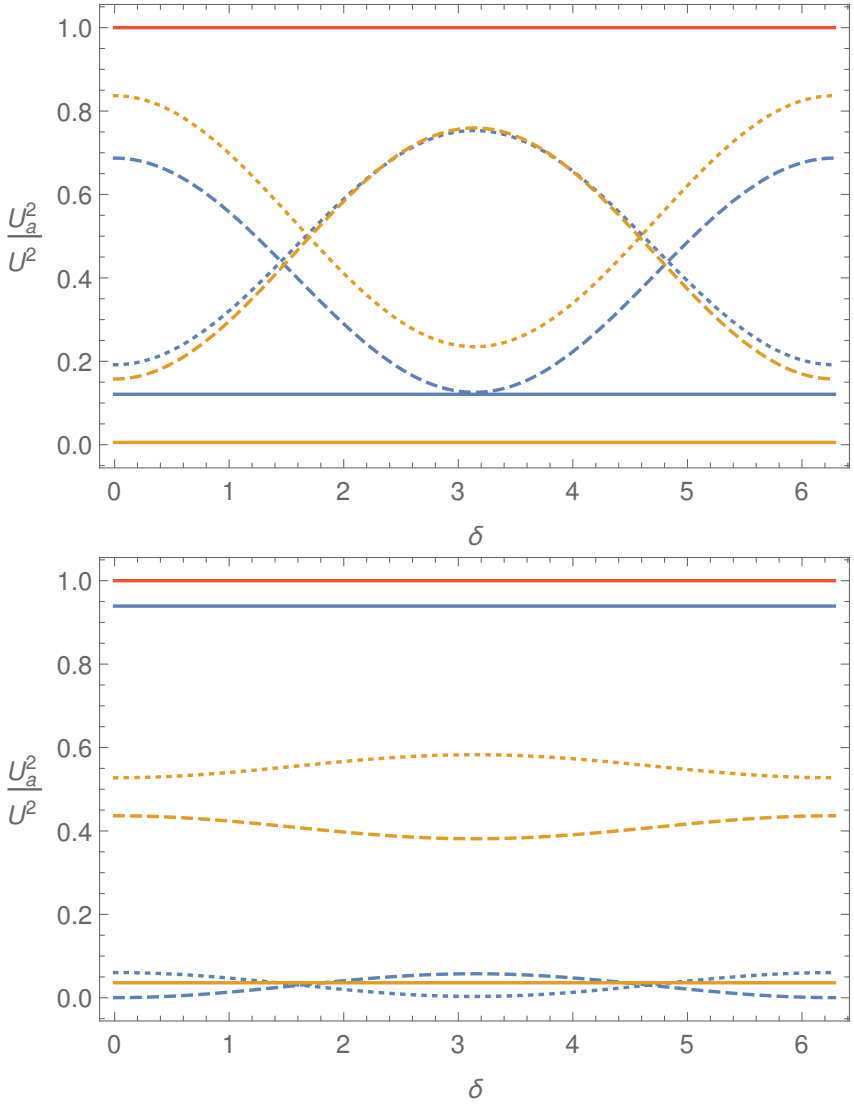

Figure 11: *Relative mixing* U_a^2/U^2 *over* δ *with* $a = e, \mu, \tau$ *for* $n_s = 2$ *sterile flavors in the limit of large* $\mathrm{Im}\omega$, *cf. Eq. (8). The electron mixings are given by solid lines, the muon mixings by dashed and the tauon mixings by dotted lines. The red line corresponds to the total mixing* $U^2 = \sum_a U_a^2$. *The upper panel assumes normal hierarchy, where the orange and blue curves indicate the cases* $\alpha_2 = -2\delta + \pi$ *and* $\alpha_2 = -2\delta + 3\pi$, *respectively. The lower panel corresponds to inverted hierarchy, where the blue and orange curves indicate the cases* $\alpha_2 = \pi$ *and* $\alpha_2 = -\pi$, *respectively.*

Inverted hierarchy:

$$U_e^2 \approx \frac{e^{2\mathrm{Im}\omega}}{2\bar{M}}\left[b_1 + b_2 \sin\left(\frac{\tilde{\alpha}}{2}\right)\right], \tag{65a}$$

$$U_\mu^2 \approx \frac{e^{2\mathrm{Im}\omega}}{2\bar{M}}\left[b_3 - b_4\cos(\delta) - b_5 \sin\left(\frac{\tilde{\alpha}}{2}\right) - b_6 \sin\left(\frac{\tilde{\alpha}}{2} - \delta\right) + b_7 \sin\left(\frac{\tilde{\alpha}}{2} + \delta\right)\right], \tag{65b}$$

$$U_\tau^2 \approx \frac{e^{2\mathrm{Im}\omega}}{2\bar{M}}\left[b_8 + b_9\cos(\delta) - b_{10} \sin\left(\frac{\tilde{\alpha}}{2}\right) + b_{11} \sin\left(\frac{\tilde{\alpha}}{2} - \delta\right) - b_{12} \sin\left(\frac{\tilde{\alpha}}{2} + \delta\right)\right], \tag{65c}$$

with a_1 to a_{12} positive real numbers given by the active neutrino masses and mixings

$$\begin{aligned}
b_1 &= m_1 c_{12}^2 c_{13}^2 + m_2 s_{12}^2\,,\\
b_2 &= 2\sqrt{m_1 m_2} c_{12} s_{12} \xi\,,\\
b_3 &= m_1(c_{23}^2 s_{12}^2 + c_{12}^2 s_{13}^2 s_{23}^2) + m_2(c_{12}^2 c_{23}^2 + s_{12}^2 s_{13}^2 s_{23}^2)\,,\\
b_4 &= 2(m_2 - m_1) c_{12} c_{23} s_{12} s_{13} s_{23}\,,\\
b_5 &= 2\sqrt{m_1 m_2}(c_{12} c_{23}^2 s_{12} - c_{12} s_{12} s_{13}^2 s_{23}^2)\xi\,,\\
b_6 &= 2\sqrt{m_1 m_2} c_{12}^2 c_{23} s_{13} s_{23} \xi\,,\\
b_7 &= 2\sqrt{m_1 m_2} c_{23} s_{12}^2 s_{13} s_{23} \xi\,,\\
b_8 &= m_1(c_{12}^2 c_{23}^2 s_{13}^2 + s_{12}^2 s_{23}^2) + m_2(c_{23}^2 s_{12}^2 s_{13}^2 + c_{12}^2 s_{23}^2)\,,\\
b_9 &= b_4\,,\\
b_{10} &= 2\sqrt{m_1 m_2}(c_{12} s_{12} s_{23}^2 - c_{12} c_{23}^2 s_{12} s_{13}^2)\xi\,,\\
b_{11} &= b_6\,,\\
b_{12} &= b_7\,,
\end{aligned} \tag{66}$$

and $\tilde{\alpha} = \alpha_2 - \alpha_1$. This implies that for inverted hierarchy the Yukawa matrices Y do only depend on the difference $\alpha_2 - \alpha_1$, which allows us to set $\alpha_1 = 0$ and take α_2 as the running parameter. In case of inverted ordering it is the maximal electron (relative) mixing $U_e^2/U^2 = 0.939$, given for $\alpha_2 = \pi$, that maximises U^2 given the leptogenesis constraints. The maximal U_μ^2/U^2 and U_τ^2/U^2 for this value of α_2 are given for $\delta = \pi$ and $\delta = 0$, respectively. The bottom panel of Figure 11 shows the relative mixings for inverted hierarchy. There we can see that maximal muon mixing corresponds to minimal tauon mixing and vice versa. The results from Eqs. (63) and (65) are consistent with previous results from Ref. [46] and lead to the approximated expressions (25)-(27).

References

[1] P. Minkowski, $\mu \to e\gamma$ at a Rate of One Out of 10^9 Muon Decays?, Phys. Lett. B67 (1977) 421–428. doi:10.1016/0370-2693(77)90435-X.

[2] M. Gell-Mann, P. Ramond, R. Slansky, Complex Spinors and Unified Theories, Conf. Proc. C790927 (1979) 315–321. arXiv:1306.4669.

[3] R. N. Mohapatra, G. Senjanovic, Neutrino Mass and Spontaneous Parity Violation, Phys. Rev. Lett. 44 (1980) 912. doi:10.1103/PhysRevLett.44.912.

[4] T. Yanagida, Horizontal Symmetry and Masses of Neutrinos, Prog. Theor. Phys. 64 (1980) 1103. doi:10.1143/PTP.64.1103.

[5] J. Schechter, J. W. F. Valle, Neutrino Masses in SU(2) x U(1) Theories, Phys. Rev. D22 (1980) 2227. doi:10.1103/PhysRevD.22.2227.

[6] J. Schechter, J. W. F. Valle, Neutrino Decay and Spontaneous Violation of Lepton Number, Phys. Rev. D25 (1982) 774. doi:10.1103/PhysRevD.25.774.

[7] A. Atre, T. Han, S. Pascoli, B. Zhang, The Search for Heavy Majorana Neutrinos, JHEP 05 (2009) 030. arXiv:0901.3589, doi:10.1088/1126-6708/2009/05/030.

[8] A. Ibarra, E. Molinaro, S. T. Petcov, Low Energy Signatures of the TeV Scale See-Saw Mechanism, Phys. Rev. D84 (2011) 013005. arXiv:1103.6217, doi:10.1103/PhysRevD.84.013005.

[9] M. Drewes, The Phenomenology of Right Handed Neutrinos, Int. J. Mod. Phys. E22 (2013) 1330019. arXiv:1303.6912, doi:10.1142/S0218301313300191.

[10] P. Hernandez, M. Kekic, J. Lopez-Pavon, $N_{\rm eff}$ in low-scale seesaw models versus the lightest neutrino mass, Phys. Rev. D90 (6) (2014) 065033. arXiv:1406.2961, doi:10.1103/PhysRevD.90.065033.

[11] S. Antusch, O. Fischer, Non-unitarity of the leptonic mixing matrix: Present bounds and future sensitivities, JHEP 10 (2014) 094. arXiv:1407.6607, doi:10.1007/JHEP10(2014)094.

[12] D. Gorbunov, I. Timiryasov, Testing νMSM with indirect searches, Phys. Lett. B745 (2015) 29–34. arXiv:1412.7751, doi:10.1016/j.physletb.2015.02.060.

[13] M. Drewes, B. Garbrecht, Experimental and cosmological constraints on heavy neutrinosarXiv:1502.00477.

[14] A. de Gouva, A. Kobach, Global Constraints on a Heavy Neutrino, Phys. Rev. D93 (3) (2016) 033005. arXiv:1511.00683, doi:10.1103/PhysRevD.93.033005.

[15] E. Fernandez-Martinez, J. Hernandez-Garcia, J. Lopez-Pavon, Global constraints on heavy neutrino mixing, JHEP 08 (2016) 033. arXiv:1605.08774, doi:10.1007/JHEP08(2016)033.

[16] F. Vissani, Do experiments suggest a hierarchy problem?, Phys. Rev. D57 (1998) 7027–7030. arXiv:hep-ph/9709409, doi:10.1103/PhysRevD.57.7027.

[17] F. Bezrukov, M. Yu. Kalmykov, B. A. Kniehl, M. Shaposhnikov, Higgs Boson Mass and New Physics, JHEP 10 (2012) 140, [,275(2012)]. arXiv:1205.2893, doi:10.1007/JHEP10(2012)140.

[18] T. Asaka, M. Shaposhnikov, The nuMSM, dark matter and baryon asymmetry of the universe, Phys. Lett. B620 (2005) 17–26. arXiv:hep-ph/0505013, doi:10.1016/j.physletb.2005.06.020.

[19] T. Asaka, S. Blanchet, M. Shaposhnikov, The nuMSM, dark matter and neutrino masses, Phys. Lett. B631 (2005) 151–156. arXiv:hep-ph/0503065, doi:10.1016/j.physletb.2005.09.070.

[20] A. Boyarsky, O. Ruchayskiy, M. Shaposhnikov, The Role of sterile neutrinos in cosmology and astrophysics, Ann. Rev. Nucl. Part. Sci. 59 (2009) 191–214. arXiv:0901.0011, doi:10.1146/annurev.nucl.010909.083654.

[21] L. Canetti, M. Drewes, T. Frossard, M. Shaposhnikov, Dark Matter, Baryogenesis and Neutrino Oscillations from Right Handed Neutrinos, Phys. Rev. D87 (2013) 093006. arXiv:1208.4607, doi:10.1103/PhysRevD.87.093006.

[22] V. V. Khoze, G. Ro, Leptogenesis and Neutrino Oscillations in the Classically Conformal Standard Model with the Higgs Portal, JHEP 10 (2013) 075. arXiv:1307.3764, doi:10.1007/JHEP10(2013)075.

[23] R. N. Mohapatra, J. W. F. Valle, Neutrino Mass and Baryon Number Nonconservation in Superstring Models, Phys. Rev. D34 (1986) 1642. doi:10.1103/PhysRevD.34.1642.

[24] R. N. Mohapatra, Mechanism for Understanding Small Neutrino Mass in Superstring Theories, Phys. Rev. Lett. 56 (1986) 561–563. doi:10.1103/PhysRevLett.56.561.

[25] Y. Chikashige, R. N. Mohapatra, R. D. Peccei, Are There Real Goldstone Bosons Associated with Broken Lepton Number?, Phys. Lett. B98 (1981) 265–268. doi:10.1016/0370-2693(81)90011-3.

[26] G. B. Gelmini, M. Roncadelli, Left-Handed Neutrino Mass Scale and Spontaneously Broken Lepton Number, Phys. Lett. B99 (1981) 411–415. doi:10.1016/0370-2693(81)90559-1.

[27] D. Wyler, L. Wolfenstein, Massless Neutrinos in Left-Right Symmetric Models, Nucl. Phys. B218 (1983) 205–214. doi:10.1016/0550-3213(83)90482-0.

[28] M. C. Gonzalez-Garcia, J. W. F. Valle, Fast Decaying Neutrinos and Observable Flavor Violation in a New Class of Majoron Models, Phys. Lett. B216 (1989) 360–366. doi:10.1016/0370-2693(89)91131-3.

[29] G. C. Branco, W. Grimus, L. Lavoura, The Seesaw Mechanism in the Presence of a Conserved Lepton Number, Nucl. Phys. B312 (1989) 492–508. doi:10.1016/0550-3213(89)90304-0.

[30] A. Abada, C. Biggio, F. Bonnet, M. B. Gavela, T. Hambye, Low energy effects of neutrino masses, JHEP 12 (2007) 061. arXiv:0707.4058, doi:10.1088/1126-6708/2007/12/061.

[31] M. Shaposhnikov, A Possible symmetry of the nuMSM, Nucl. Phys. B763 (2007) 49–59. arXiv:hep-ph/0605047, doi:10.1016/j.nuclphysb.2006.11.003.

[32] M. B. Gavela, T. Hambye, D. Hernandez, P. Hernandez, Minimal Flavour Seesaw Models, JHEP 09 (2009) 038. arXiv:0906.1461, doi:10.1088/1126-6708/2009/09/038.

[33] D. Aristizabal Sierra, A. Degee, J. F. Kamenik, Minimal Lepton Flavor Violating Realizations of Minimal Seesaw Models, JHEP 07 (2012) 135. arXiv:1205.5547, doi:10.1007/JHEP07(2012)135.

[34] J. Racker, M. Pena, N. Rius, Leptogenesis with small violation of B-L, JCAP 1207 (2012) 030. arXiv:1205.1948, doi:10.1088/1475-7516/2012/07/030.

[35] C. S. Fong, M. C. Gonzalez-Garcia, E. Nardi, E. Peinado, New ways to TeV scale leptogenesis, JHEP 08 (2013) 104. arXiv:1305.6312, doi:10.1007/JHEP08(2013)104.

[36] L. Canetti, M. Drewes, M. Shaposhnikov, Matter and Antimatter in the Universe, New J. Phys. 14 (2012) 095012. arXiv:1204.4186, doi:10.1088/1367-2630/14/9/095012.

[37] E. K. Akhmedov, V. A. Rubakov, A. Yu. Smirnov, Baryogenesis via neutrino oscillations, Phys. Rev. Lett. 81 (1998) 1359–1362. arXiv:hep-ph/9803255, doi:10.1103/PhysRevLett.81.1359.

[38] M. Fukugita, T. Yanagida, Baryogenesis Without Grand Unification, Phys. Lett. B174 (1986) 45–47. doi:10.1016/0370-2693(86)91126-3.

[39] R. Adhikari, et al., A White Paper on keV Sterile Neutrino Dark Matter, Submitted to: White paperarXiv:1602.04816.

[40] M. Shaposhnikov, Is there a new physics between electroweak and Planck scales?, in: Astroparticle Physics: Current Issues, 2007 (APCI07) Budapest, Hungary, June 21-23, 2007, 2007. arXiv:0708.3550.
URL https://inspirehep.net/record/759157/files/arXiv:0708.3550.pdf

[41] R. E. Shrock, General Theory of Weak Leptonic and Semileptonic Decays. 1. Leptonic Pseudoscalar Meson Decays, with Associated Tests For, and Bounds on, Neutrino Masses and Lepton Mixing, Phys. Rev. D24 (1981) 1232. doi:10.1103/PhysRevD.24.1232.

[42] R. E. Shrock, General Theory of Weak Processes Involving Neutrinos. 2. Pure Leptonic Decays, Phys. Rev. D24 (1981) 1275. doi:10.1103/PhysRevD.24.1275.

[43] M. C. Gonzalez-Garcia, M. Maltoni, T. Schwetz, Updated fit to three neutrino mixing: status of leptonic CP violation, JHEP 11 (2014) 052. arXiv:1409.5439, doi:10.1007/JHEP11(2014)052.

[44] T. Asaka, S. Eijima, H. Ishida, Mixing of Active and Sterile Neutrinos, JHEP 04 (2011) 011. arXiv:1101.1382, doi:10.1007/JHEP04(2011)011.

[45] O. Ruchayskiy, A. Ivashko, Experimental bounds on sterile neutrino mixing angles, JHEP 06 (2012) 100. arXiv:1112.3319, doi:10.1007/JHEP06(2012)100.

[46] P. Hernndez, M. Kekic, J. Lpez-Pavn, J. Racker, J. Salvado, Testable Baryogenesis in Seesaw Models, JHEP 08 (2016) 157. arXiv:1606.06719, doi:10.1007/JHEP08(2016)157.

[47] J. A. Casas, A. Ibarra, Oscillating neutrinos and muon —¿ e, gamma, Nucl. Phys. B618 (2001) 171–204. arXiv:hep-ph/0103065, doi:10.1016/S0550-3213(01)00475-8.

[48] J. Lopez-Pavon, E. Molinaro, S. T. Petcov, Radiative Corrections to Light Neutrino Masses in Low Scale Type I Seesaw Scenarios and Neutrinoless Double Beta Decay, JHEP 11 (2015) 030. arXiv:1506.05296, doi:10.1007/JHEP11(2015)030.

[49] M. Drewes, S. Eijima, Neutrinoless double β decay and low scale leptogenesisarXiv:1606.06221.

[50] M. Drewes, B. Garbrecht, Leptogenesis from a GeV Seesaw without Mass Degeneracy, JHEP 03 (2013) 096. arXiv:1206.5537, doi:10.1007/JHEP03(2013)096.

[51] M. Anelli, et al., A facility to Search for Hidden Particles (SHiP) at the CERN SPSarXiv:1504.04956.

[52] S. Alekhin, et al., A facility to Search for Hidden Particles at the CERN SPS: the SHiP physics casearXiv:1504.04855.

[53] K. N. Abazajian, et al., Light Sterile Neutrinos: A White PaperarXiv:1204.5379.

[54] E. Fernandez-Martinez, J. Hernandez-Garcia, J. Lopez-Pavon, M. Lucente, Loop level constraints on Seesaw neutrino mixing, JHEP 10 (2015) 130. arXiv:1508.03051, doi:10.1007/JHEP10(2015)130.

[55] F. J. Escrihuela, D. V. Forero, O. G. Miranda, M. Tortola, J. W. F. Valle, On the description of nonunitary neutrino mixing, Phys. Rev. D92 (5) (2015) 053009, [Erratum: Phys. Rev.D93,no.11,119905(2016)]. arXiv:1503.08879, doi:10.1103/PhysRevD.93.119905,10.1103/PhysRevD.92.053009.

[56] F. F. Deppisch, P. S. Bhupal Dev, A. Pilaftsis, Neutrinos and Collider Physics, New J. Phys. 17 (7) (2015) 075019. arXiv:1502.06541, doi:10.1088/1367-2630/17/7/075019.

[57] P. Abreu, et al., Search for neutral heavy leptons produced in Z decays, Z. Phys. C74 (1997) 57–71, [Erratum: Z. Phys.C75,580(1997)]. doi:10.1007/s002880050370.

[58] O. Adriani, et al., Search for isosinglet neutral heavy leptons in Z0 decays, Phys. Lett. B295 (1992) 371–382. doi:10.1016/0370-2693(92)91579-X.

[59] R. Aaij, et al., Search for Majorana neutrinos in $B^- \to \pi^+\mu^-\mu^-$ decays, Phys. Rev. Lett. 112 (13) (2014) 131802. arXiv:1401.5361, doi:10.1103/PhysRevLett.112.131802.

[60] G. Aad, et al., Search for heavy Majorana neutrinos with the ATLAS detector in pp collisions at $\sqrt{s} = 8$ TeV, JHEP 07 (2015) 162. arXiv:1506.06020, doi:10.1007/JHEP07(2015)162.

[61] V. Khachatryan, et al., Search for heavy Majorana neutrinos in $\mu^\pm\mu^\pm$+ jets events in proton-proton collisions at $\sqrt{s} = 8$ TeV, Phys. Lett. B748 (2015) 144–166. arXiv:1501.05566, doi:10.1016/j.physletb.2015.06.070.

[62] D. Liventsev, et al., Search for heavy neutrinos at Belle, Phys. Rev. D87 (7) (2013) 071102. arXiv:1301.1105, doi:10.1103/PhysRevD.87.071102.

[63] A. M. Cooper-Sarkar, et al., Search for Heavy Neutrino Decays in the BEBC Beam Dump Experiment, Phys. Lett. B160 (1985) 207–211. doi:10.1016/0370-2693(85)91493-5.

[64] E. Gallas, et al., Search for neutral weakly interacting massive particles in the Fermilab Tevatron wide band neutrino beam, Phys. Rev. D52 (1995) 6–14. doi:10.1103/PhysRevD.52.6.

[65] A. V. Artamonov, et al., Search for heavy neutrinos in $K^+ \to \mu^+\nu_H$ decays, Phys. Rev. D91 (5) (2015) 052001, [Erratum: Phys. Rev.D91,no.5,059903(2015)]. arXiv:1411.3963, doi:10.1103/PhysRevD.91.059903,10.1103/PhysRevD.91.052001.

[66] M. Aoki, et al., Search for Massive Neutrinos in the Decay $\pi \to e\nu$, Phys. Rev. D84 (2011) 052002. arXiv:1106.4055, doi:10.1103/PhysRevD.84.052002.

[67] P. Astier, et al., Search for heavy neutrinos mixing with tau neutrinos, Phys. Lett. B506 (2001) 27–38. arXiv:hep-ex/0101041, doi:10.1016/S0370-2693(01)00362-8.

[68] D. I. Britton, et al., Improved search for massive neutrinos in pi+ —¿ e+ neutrino decay, Phys. Rev. D46 (1992) R885–R887. doi:10.1103/PhysRevD.46.R885.

[69] G. Bernardi, et al., FURTHER LIMITS ON HEAVY NEUTRINO COUPLINGS, Phys. Lett. B203 (1988) 332–334. doi:10.1016/0370-2693(88)90563-1.

[70] F. Bergsma, et al., A Search for Decays of Heavy Neutrinos in the Mass Range 0.5-GeV to 2.8-GeV, Phys. Lett. B166 (1986) 473–478. doi:10.1016/0370-2693(86)91601-1.

[71] J. Orloff, A. N. Rozanov, C. Santoni, Limits on the mixing of tau neutrino to heavy neutrinos, Phys. Lett. B550 (2002) 8–15. arXiv:hep-ph/0208075, doi:10.1016/S0370-2693(02)02769-7.

[72] P. Vilain, et al., Search for heavy isosinglet neutrinos, Phys. Lett. B343 (1995) 453–458, [Phys. Lett.B351,387(1995)]. doi:10.1016/0370-2693(94)00440-I,10.1016/0370-2693(94)01422-9.

[73] A. Vaitaitis, et al., Search for neutral heavy leptons in a high-energy neutrino beam, Phys. Rev. Lett. 83 (1999) 4943–4946. arXiv:hep-ex/9908011, doi:10.1103/PhysRevLett.83.4943.

[74] J. Badier, et al., Direct Photon Production From Pions and Protons at 200-GeV/c, Z. Phys. C31 (1986) 341. doi:10.1007/BF01588030.

[75] T. Yamazaki, et al., Search for Heavy Neutrinos in Kaon Decay (1984) I.262[Conf. Proc.C840719,262(1984)].

[76] R. S. Hayano, et al., HEAVY NEUTRINO SEARCH USING K(mu2) DECAY, Phys. Rev. Lett. 49 (1982) 1305. doi:10.1103/PhysRevLett.49.1305.

[77] M. Agostini, et al., Results on Neutrinoless Double-β Decay of ^{76}Ge from Phase I of the GERDA Experiment, Phys. Rev. Lett. 111 (12) (2013) 122503. arXiv:1307.4720, doi:10.1103/PhysRevLett.111.122503.

[78] A. Gando, et al., Search for Majorana Neutrinos near the Inverted Mass Hierarchy Region with KamLAND-Zen, Phys. Rev. Lett. 117 (8) (2016) 082503, [Addendum: Phys. Rev. Lett.117,no.10,109903(2016)]. arXiv:1605.02889, doi:10.1103/PhysRevLett.117.109903,10.1103/PhysRevLett.117.082503.

[79] C. Lazzeroni, et al., Precision Measurement of the Ratio of the Charged Kaon Leptonic Decay Rates, Phys. Lett. B719 (2013) 326–336. arXiv:1212.4012, doi:10.1016/j.physletb.2013.01.037.

[80] G. Czapek, et al., Branching ratio for the rare pion decay into positron and neutrino, Phys. Rev. Lett. 70 (1993) 17–20. doi:10.1103/PhysRevLett.70.17.

[81] J. Beringer, et al., Review of Particle Physics (RPP), Phys. Rev. D86 (2012) 010001. doi:10.1103/PhysRevD.86.010001.

[82] M. Antonelli, et al., An Evaluation of $|V_{us}|$ and precise tests of the Standard Model from world data on leptonic and semileptonic kaon decays, Eur. Phys. J. C69 (2010) 399–424. arXiv:1005.2323, doi:10.1140/epjc/s10052-010-1406-3.

[83] S. Aoki, et al., Review of lattice results concerning low-energy particle physics, Eur. Phys. J. C74 (2014) 2890. arXiv:1310.8555, doi:10.1140/epjc/s10052-014-2890-7.

[84] E. Follana, C. T. H. Davies, G. P. Lepage, J. Shigemitsu, High Precision determination of the pi, K, D and D(s) decay constants from lattice QCD, Phys. Rev. Lett. 100 (2008) 062002. arXiv:0706.1726, doi:10.1103/PhysRevLett.100.062002.

[85] Y. Amhis, et al., Averages of B-Hadron, C-Hadron, and tau-lepton properties as of early 2012arXiv:1207.1158.

[86] J. Adam, et al., New constraint on the existence of the $\mu^+ \to e^+\gamma$ decay, Phys. Rev. Lett. 110 (2013) 201801. arXiv:1303.0754, doi:10.1103/PhysRevLett.110.201801.

[87] G. Blankenburg, J. Ellis, G. Isidori, Flavour-Changing Decays of a 125 GeV Higgs-like Particle, Phys. Lett. B712 (2012) 386–390. arXiv:1202.5704, doi:10.1016/j.physletb.2012.05.007.

[88] M. Baak, J. Cth, J. Haller, A. Hoecker, R. Kogler, K. Mnig, M. Schott, J. Stelzer, The global electroweak fit at NNLO and prospects for the LHC and ILC, Eur. Phys. J. C74 (2014) 3046. arXiv:1407.3792, doi:10.1140/epjc/s10052-014-3046-5.

[89] S. Schael, et al., Precision electroweak measurements on the Z resonance, Phys. Rept. 427 (2006) 257–454. arXiv:hep-ex/0509008, doi:10.1016/j.physrep.2005.12.006.

[90] T. E. W. Group, 2012 Update of the Combination of CDF and D0 Results for the Mass of the W BosonarXiv:1204.0042.

[91] A. Ferroglia, A. Sirlin, Comparison of the standard theory predictions of M_W and $\sin{}^2\theta^{lept}_{eff}$ with their experimental values, Phys. Rev. D87 (3) (2013) 037501. arXiv:1211.1864, doi:10.1103/PhysRevD.87.037501.

[92] D. Gorbunov, M. Shaposhnikov, How to find neutral leptons of the νMSM?, JHEP 10 (2007) 015, [Erratum: JHEP11,101(2013)]. arXiv:0705.1729, doi:10.1007/JHEP11(2013)101,10.1088/1126-6708/2007/10/015.

[93] P. Hernandez, M. Kekic, J. Lopez-Pavon, Low-scale seesaw models versus N_{eff}, Phys. Rev. D89 (7) (2014) 073009. arXiv:1311.2614, doi:10.1103/PhysRevD.89.073009.

[94] O. Ruchayskiy, A. Ivashko, Restrictions on the lifetime of sterile neutrinos from primordial nucleosynthesis, JCAP 1210 (2012) 014. arXiv:1202.2841, doi:10.1088/1475-7516/2012/10/014.

[95] L. Canetti, M. Shaposhnikov, The ν MSM and muon to electron conversion experiments, Hyperfine Interact. 214 (1-3) (2013) 5–11. doi:10.1007/s10751-013-0796-7.

[96] M. Shaposhnikov, The nuMSM, leptonic asymmetries, and properties of singlet fermions, JHEP 08 (2008) 008. arXiv:0804.4542, doi:10.1088/1126-6708/2008/08/008.

[97] M. Laine, M. Shaposhnikov, Sterile neutrino dark matter as a consequence of nuMSM-induced lepton asymmetry, JCAP 0806 (2008) 031. arXiv:0804.4543, doi:10.1088/1475-7516/2008/06/031.

[98] X.-D. Shi, G. M. Fuller, A New dark matter candidate: Nonthermal sterile neutrinos, Phys. Rev. Lett. 82 (1999) 2832–2835. arXiv:astro-ph/9810076, doi:10.1103/PhysRevLett.82.2832.

[99] A. Roy, M. Shaposhnikov, Resonant production of the sterile neutrino dark matter and fine-tunings in the [nu]MSM, Phys. Rev. D82 (2010) 056014. arXiv:1006.4008, doi:10.1103/PhysRevD.82.056014.

[100] G. Cveti, C. S. Kim, J. Zamora-Sa, CP violation in lepton number violating semihadronic decays of K, D, D_s, B, B_c, Phys. Rev. D89 (9) (2014) 093012. arXiv:1403.2555, doi:10.1103/PhysRevD.89.093012.

[101] G. Cvetic, C. Dib, C. S. Kim, J. Zamora-Saa, Probing the Majorana neutrinos and their CP violation in decays of charged scalar mesons π, K, D, D_s, B, B_c, Symmetry 7 (2015) 726–773. arXiv:1503.01358, doi:10.3390/sym7020726.

[102] G. Cvetic, C. S. Kim, R. Kogerler, J. Zamora-Saa, Oscillation of heavy sterile neutrino in decay of $B \to \mu e \pi$, Phys. Rev. D92 (2015) 013015. arXiv:1505.04749, doi:10.1103/PhysRevD.92.013015.

[103] D. Boyanovsky, Nearly degenerate heavy sterile neutrinos in cascade decay: mixing and oscillations, Phys. Rev. D90 (10) (2014) 105024. arXiv:1409.4265, doi:10.1103/PhysRevD.90.105024.

[104] C. O. Dib, C. S. Kim, K. Wang, J. Zhang, Distinguishing Dirac/Majorana Sterile Neutrinos at the LHC, Phys. Rev. D94 (1) (2016) 013005. arXiv:1605.01123, doi:10.1103/PhysRevD.94.013005.

[105] C. O. Dib, C. S. Kim, Discovering sterile Neutrinos ligther than M_W at the LHC, Phys. Rev. D92 (9) (2015) 093009. arXiv:1509.05981, doi:10.1103/PhysRevD.92.093009.

[106] G. Anamiati, M. Hirsch, E. Nardi, Quasi-Dirac neutrinos at the LHCarXiv:1607.05641.

[107] V. A. Kuzmin, V. A. Rubakov, M. E. Shaposhnikov, On the Anomalous Electroweak Baryon Number Nonconservation in the Early Universe, Phys. Lett. B155 (1985) 36. doi:10.1016/0370-2693(85)91028-7.

[108] M. D'Onofrio, K. Rummukainen, A. Tranberg, Sphaleron Rate in the Minimal Standard Model, Phys. Rev. Lett. 113 (14) (2014) 141602. arXiv:1404.3565, doi:10.1103/PhysRevLett.113.141602.

[109] A. Anisimov, W. Buchmller, M. Drewes, S. Mendizabal, Quantum Leptogenesis I, Annals Phys. 326 (2011) 1998–2038, [Erratum: Annals Phys.338,376(2011)]. arXiv:1012.5821, doi:10.1016/j.aop.2011.02.002,10.1016/j.aop.2013.05.00.

[110] A. Anisimov, W. Buchmuller, M. Drewes, S. Mendizabal, Leptogenesis from Quantum Interference in a Thermal Bath, Phys. Rev. Lett. 104 (2010) 121102. arXiv:1001.3856, doi:10.1103/PhysRevLett.104.121102.

[111] L. Canetti, M. Shaposhnikov, Baryon Asymmetry of the Universe in the NuMSM, JCAP 1009 (2010) 001. arXiv:1006.0133, doi:10.1088/1475-7516/2010/09/001.

[112] M. Garny, A. Kartavtsev, A. Hohenegger, Leptogenesis from first principles in the resonant regime, Annals Phys. 328 (2013) 26–63. arXiv:1112.6428, doi:10.1016/j.aop.2012.10.007.

[113] B. Garbrecht, M. Herranen, Effective Theory of Resonant Leptogenesis in the Closed-Time-Path Approach, Nucl. Phys. B861 (2012) 17–52. arXiv:1112.5954, doi:10.1016/j.nuclphysb.2012.03.009.

[114] L. Canetti, M. Drewes, M. Shaposhnikov, Sterile Neutrinos as the Origin of Dark and Baryonic Matter, Phys. Rev. Lett. 110 (6) (2013) 061801. arXiv:1204.3902, doi:10.1103/PhysRevLett.110.061801.

[115] L. Canetti, M. Drewes, B. Garbrecht, Probing leptogenesis with GeV-scale sterile neutrinos at LHCb and Belle II, Phys. Rev. D90 (12) (2014) 125005. arXiv:1404.7114, doi:10.1103/PhysRevD.90.125005.

[116] B. Shuve, I. Yavin, Baryogenesis through Neutrino Oscillations: A Unified Perspective, Phys. Rev. D89 (7) (2014) 075014. arXiv:1401.2459, doi:10.1103/PhysRevD.89.075014.

[117] B. Garbrecht, More Viable Parameter Space for Leptogenesis, Phys. Rev. D90 (6) (2014) 063522. arXiv:1401.3278, doi:10.1103/PhysRevD.90.063522.

[118] A. Abada, G. Arcadi, V. Domcke, M. Lucente, Lepton number violation as a key to low-scale leptogenesis, JCAP 1511 (11) (2015) 041. arXiv:1507.06215, doi:10.1088/1475-7516/2015/11/041.

[119] P. Hernndez, M. Kekic, J. Lpez-Pavn, J. Racker, N. Rius, Leptogenesis in GeV scale seesaw models, JHEP 10 (2015) 067. arXiv:1508.03676, doi:10.1007/JHEP10(2015)067.

[120] A. Kartavtsev, P. Millington, H. Vogel, Lepton asymmetry from mixing and oscillations, JHEP 06 (2016) 066. arXiv:1601.03086, doi:10.1007/JHEP06(2016)066.

[121] M. Drewes, B. Garbrecht, D. Gueter, J. Klaric, Leptogenesis from Oscillations of Heavy Neutrinos with Large Mixing AnglesarXiv:1606.06690.

[122] T. Hambye, D. Teresi, Higgs doublet decay as the origin of the baryon asymmetry, Phys. Rev. Lett. 117 (9) (2016) 091801. arXiv:1606.00017, doi:10.1103/PhysRevLett.117.091801.

[123] B. Garbrecht, F. Glowna, P. Schwaller, Scattering Rates For Leptogenesis: Damping of Lepton Flavour Coherence and Production of Singlet Neutrinos, Nucl. Phys. B877 (2013) 1–35. arXiv:1303.5498, doi:10.1016/j.nuclphysb.2013.08.020.

[124] D. Besak, D. Bodeker, Thermal production of ultrarelativistic right-handed neutrinos: Complete leading-order results, JCAP 1203 (2012) 029. arXiv:1202.1288, doi:10.1088/1475-7516/2012/03/029.

[125] I. Ghisoiu, M. Laine, Right-handed neutrino production rate at T ¿ 160 GeV, JCAP 1412 (12) (2014) 032. arXiv:1411.1765, doi:10.1088/1475-7516/2014/12/032.

[126] M. Laine, Thermal right-handed neutrino production rate in the relativistic regime, JHEP 08 (2013) 138. arXiv:1307.4909, doi:10.1007/JHEP08(2013)138.

[127] G. Sigl, G. Raffelt, General kinetic description of relativistic mixed neutrinos, Nucl. Phys. B406 (1993) 423–451. doi:10.1016/0550-3213(93)90175-O.

[128] E. Graverini, SHiP sensitivity to Heavy Neutral Leptons.
URL https://cds.cern.ch/record/2214085

[129] C. Adams, et al., The Long-Baseline Neutrino Experiment: Exploring Fundamental Symmetries of the UniversearXiv:1307.7335.

[130] A. Blondel, E. Graverini, N. Serra, M. Shaposhnikov, Search for Heavy Right Handed Neutrinos at the FCC-ee, in: Proceedings, 37th International Conference on High Energy Physics (ICHEP 2014): Valencia, Spain, July 2-9, 2014, 2016. arXiv:1411.5230, doi:10.1016/j.nuclphysbps.2015.09.304.
URL https://inspirehep.net/record/1328783/files/arXiv:1411.5230.pdf

[131] S. Antusch, E. Cazzato, O. Fischer, Displaced vertex searches for sterile neutrinos at future lepton collidersarXiv:1604.02420.

[132] T. Spadaro, Perspectives from the NA62 experiment, Talk given at the PBC Kickoff Meeting - CERN (September 2016).

[133] T. Asaka, H. Ishida, Lepton number violation by heavy Majorana neutrino in B decaysarXiv:1609.06113.

[134] E. Izaguirre, B. Shuve, Multilepton and Lepton Jet Probes of Sub-Weak-Scale Right-Handed Neutrinos, Phys. Rev. D91 (9) (2015) 093010. arXiv:1504.02470, doi:10.1103/PhysRevD.91.093010.

[135] A. Kobach, S. Dobbs, Heavy Neutrinos and the Kinematics of Tau Decays, Phys. Rev. D91 (5) (2015) 053006. arXiv:1412.4785, doi:10.1103/PhysRevD.91.053006.

[136] P. A. R. Ade, et al., Planck 2015 results. XIII. Cosmological parameters, Astron. Astrophys. 594 (2016) A13. arXiv:1502.01589, doi:10.1051/0004-6361/201525830.

[137] J. C. Helo, M. Hirsch, S. Kovalenko, Heavy neutrino searches at the LHC with displaced vertices, Phys. Rev. D89 (2014) 073005, [Erratum: Phys. Rev.D93,no.9,099902(2016)]. arXiv:1312.2900, doi:10.1103/PhysRevD.89.073005,10.1103/PhysRevD.93.099902.

[138] A. M. Gago, P. Hernndez, J. Jones-Prez, M. Losada, A. Moreno Briceo, Probing the Type I Seesaw Mechanism with Displaced Vertices at the LHC, Eur. Phys. J. C75 (10) (2015) 470. arXiv:1505.05880, doi:10.1140/epjc/s10052-015-3693-1.

[139] A. Abada, V. De Romeri, S. Monteil, J. Orloff, A. M. Teixeira, Indirect searches for sterile neutrinos at a high-luminosity Z-factory, JHEP 04 (2015) 051. arXiv:1412.6322, doi:10.1007/JHEP04(2015)051.

[140] E. Graverini, N. Serra, B. Storaci, Search for New Physics in SHiP and at future colliders, JINST 10 (07) (2015) C07007. arXiv:1503.08624, doi:10.1088/1748-0221/10/07/C07007.

[141] S. Antusch, O. Fischer, Testing sterile neutrino extensions of the Standard Model at future lepton colliders, JHEP 05 (2015) 053. arXiv:1502.05915, doi:10.1007/JHEP05(2015)053.

[142] T. Asaka, T. Tsuyuki, Seesaw mechanism at electron-electron colliders, Phys. Rev. D92 (9) (2015) 094012. arXiv:1508.04937, doi:10.1103/PhysRevD.92.094012.

[143] A. Abada, D. Beirevi, M. Lucente, O. Sumensari, Lepton flavor violating decays of vector quarkonia and of the Z boson, Phys. Rev. D91 (11) (2015) 113013. arXiv:1503.04159, doi:10.1103/PhysRevD.91.113013.

[144] J. P. Chou, D. Curtin, H. J. Lubatti, New Detectors to Explore the Lifetime FrontierarXiv:1606.06298.

[145] M. Bicer, et al., First Look at the Physics Case of TLEP, JHEP 01 (2014) 164. arXiv:1308.6176, doi:10.1007/JHEP01(2014)164.

[146] B. Shuve, M. E. Peskin, Revision of the LHCb Limit on Majorana NeutrinosarXiv:1607.04258.

[147] D. Milanes, N. Quintero, C. E. Vera, Sensitivity to Majorana neutrinos in $\Delta L = 2$ decays of B_c meson at LHCb, Phys. Rev. D93 (9) (2016) 094026. arXiv:1604.03177, doi:10.1103/PhysRevD.93.094026.

[148] T. Asaka, S. Eijima, A. Watanabe, Heavy neutrino search in accelerator-based experiments, JHEP 03 (2013) 125. arXiv:1212.1062, doi:10.1007/JHEP03(2013)125.

[149] T. Akiri, et al., The 2010 Interim Report of the Long-Baseline Neutrino Experiment Collaboration Physics Working GroupsarXiv:1110.6249.

[150] J. Lopez-Pavon, S. Pascoli, C.-f. Wong, Can heavy neutrinos dominate neutrinoless double beta decay?, Phys. Rev. D87 (9) (2013) 093007. arXiv:1209.5342, doi:10.1103/PhysRevD.87.093007.

[151] A. Faessler, M. Gonzlez, S. Kovalenko, F. imkovic, Arbitrary mass Majorana neutrinos in neutrinoless double beta decay, Phys. Rev. D90 (9) (2014) 096010. arXiv:1408.6077, doi:10.1103/PhysRevD.90.096010.

[152] T. Asaka, S. Eijima, H. Ishida, On neutrinoless double beta decay in the νMSMarXiv:1606.06686.

[153] F. L. Bezrukov, nu MSM-predictions for neutrinoless double beta decay, Phys. Rev. D72 (2005) 071303. arXiv:hep-ph/0505247, doi:10.1103/PhysRevD.72.071303.

[154] T. P. Cheng, L.-F. Li, $\mu \to e\gamma$ in Theories With Dirac and Majorana Neutrino Mass Terms, Phys. Rev. Lett. 45 (1980) 1908. doi:10.1103/PhysRevLett.45.1908.

[155] S. M. Bilenky, S. T. Petcov, B. Pontecorvo, Lepton Mixing, mu –¿ e + gamma Decay and Neutrino Oscillations, Phys. Lett. B67 (1977) 309. doi:10.1016/0370-2693(77)90379-3.

[156] T. Asaka, S. Eijima, K. Takeda, Lepton Universality in the νMSM, Phys. Lett. B742 (2015) 303–309. arXiv:1410.0432, doi:10.1016/j.physletb.2015.01.049.

[157] V. Cirigliano, I. Rosell, Two-loop effective theory analysis of pi (K) —¿ e anti-nu/e [gamma] branching ratios, Phys. Rev. Lett. 99 (2007) 231801. arXiv:0707.3439, doi:10.1103/PhysRevLett.99.231801.

[158] A. Pich, I. Boyko, D. Dedovich, I. I. Bigi, Tau decays, Int. J. Mod. Phys. A24S1 (2009) 715–737. doi:10.1142/S0217751X09046746.